AL-MUSTANSIRIYAH JOURNAL OF SCIENCE

Volume 5 No. 1, June 1980

College of SCIENCE, AL-MUSTANSIRIYAH
UNIVERSITY BAGHDAD-IRAQ

CONTENT

BASIM OFFSET PRESS

AL-MUSTANSIRIYAH JOURNAL OF SCIENCE

VOL. 5 NO. 1, 1980

College of science, Al-Mustansiriyah University Baghdad-Iraq

Instructions for Authors:

1. Manuscripts should be Submitted in triplicate, they should be typewritten with double spacings. A margin of about 2.5 cm should be left onthe left hand side.
2. Both Arabic and English abstracts should be submitted, typed on separate sheets of paper.
3. The title of the Paper together with the name and address of the author (s) should be typed on a separate sheet. Name of author shouldbe written in full e.g Ahmed M. Ali.
4. Figures and illustrations should be drawn in black china ink on tracing Papers. Three photocopies of each diagram should also be submitted. Captions to figures should be written on the trace paper.
5. Tables should be arranged in such away so as to make them legible .
6. The same facts should not be given in tables and figures except when it is absoutely necessary to do so.
7. Reference numbers should be written between square brackets []. A list of referances should be given on a separate sheet of paper.
8. Where possible, Papers should follow the Pattern: Introduction, Experimental, Results and Discussion.

AL-MUSTANSIRIYAH JOURNAL OF SCIENCE

1980

CONTENT

CONTENT

Title Page

PHOTOCHEMICAL ADDITION OF 1,3-DIOXOLANE TO D-RIBAL TRIACETATE AND SUBSEQUENT HYDROLYSIS OF THE ADDUCT.

F.B.I. Al-Bandar and Salman A.S. Al-Janabi*

INTRODUCTION

The addition of 1,3-dioxolane to the endocylclic double bond of 2,3,5-tri-O-acetyl-D-ribal (1) enhanced by photochemical radiation using either sunlight or a U.V. lamp. Subsequent acid hydrolysis of the adduct was carried out yielding a product with clear indication of the presence of free carbonyl group.

Light induced addition of 1,3-dioxolane and similar compounds to olefines have been demonstrated by Rosenthal and Elad[1]. Addition of 1,3-dioxolane to unsaturated carbohydrates was reported later [2] . Photochemical reaction products showed that 1,3-dioxolane favors addition from position (2) and less likely from position (4) [3]. A mixture of products is usually obtained indicating the most probable free radical mechanism of addition.

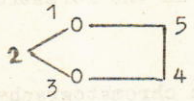

1,3-Dioxolane molecule

Hydrolysis of the 1:2 adduct was the important next step as the expected 2,5-anhydro furanose to be produced would have a free aldehyde group at C_1 which is an attractive functional group for elaboration of C-nucleosides and their analogs [4].

---

* Department of Physics, College of Education, Al-Mustansiriyah University, Baghdad - IRAQ.

Al-Mustansiriyah Journal of Science, Vol. 5, No. 1 (1979).

RESULTS AND DISCUSSION

2,3,5-tri-O-acetyl-D-ribal (1) was radiated under direct sunlight in dry acetone using quartz cell. The products were identical to the one obtained under radiation with U.V. light using a high pressure mercury lamp. When aqueous acetone was used, the reaction was found to be faster with better yields.

The photochemical addition of the 1,3-dioxolane-2-yl-radical to (1) would take place at C_1 mainly 3 from both α-and β sides of the 1-enofurancyl ring thus giving (2) and (3) in a relative ratio of 1:1.

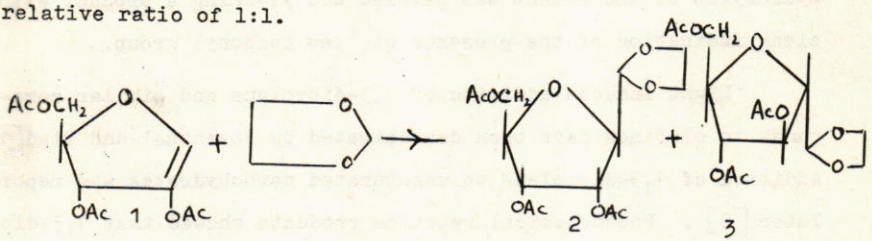

T.L.C. indicated the presence of mainly 2 spots attributed to compounds (2) and (3) and some of the starting material.

Prolonged treatment would result in the formation of deacetylated products.

Elution of the products by column chromatography afforded reasonable yields of the expected products which were identified by C,H analysis and both I.R. and N.M.R. spectroscopy.

I.R. spectroscopy indicated the absence of C=C streching in the products. N.M.R. spectroscopy indicated the absence of the chemical shift of the olefinic proton with the presence of a lower shift for aldehydic proton plus other shifts for ethylenic protons.

Acid treatment of compound (2) as an attempt to produce compound (5) was not successful due to the apparant rearrangement of (5) after deacetylation in the acidic medium 4

to give the 1,4 anhydro allose (6) which was indicated clearly by elemantel analysis on the isolated products from such treatment.

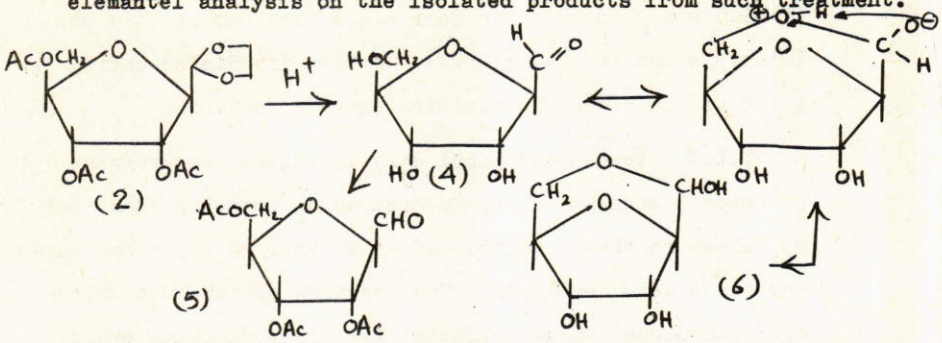

Therefore, it was important to reacetylate (4) in the reaction mixture to protect C_5 from attack using acetic anhydride and pyridine then the product after isolation was treated with aqueous acetic acid (50%) [5]. T.L.C. indicated the presence of two components. The more polar component gave a positive test with 2,4-dinitrophenyl hydrazine.

I.R. spectum of the expected aldehydic product showed the presence of acetate groups at 1745 cm^{-1}, and H-C=O stretching at 2880 cm^{-1}, while the N.M.R. data showed the presence of an indistinct doublet at δ 8.81 corresponding to aldehydic proton.

Further proof of the structure of the 1:2 adduct was achieved by its hydrolysis in sodium ethoxide to give the free alcohol, 2-β-ribofuranosyl-1,3-dioxolane which showed two significant signals at δ 4.7 and 3.7 for the acetal and methylene protons respectively by M.M.R. spectroscopy.

EXPERIMENTAL

Photolysis work:

1. Under Ultraviolat Light:

   A) By using 1,3-dioxolane and aqueous acetone:

   A mixture of 1,3-dioxolane (15 ml.), aqueous acetone (2 ml, 2%), and the D-ribal derivative (1) (1 g.) was irradiated for 24 hrs.

A solution of D-ribal derivative (1) (0.5g.) in acetone (4 ml.) was then added in four equal portions at (12) hrs intervals and the mixture was further irradiated until there was no change in reaction mixture (96) hrs.

T.L.C. (benzene:methanol 8:2) indicated the presence of three components after 36 hrs. which possesed identical R_f values to the reagents. After further 24 hours two more compounds were developed. The reaction mixture was dried over anhydrous sodium sulphate, filtered, and then evaporated to dryness. The residue (1.3 g.) was adsorbed on silica gel (150 g.) Elution with benzene afforded a fraction (0.39 g. 20% yield) which was attributed to the starting material (1) followed by a second fraction (0.8g. 47.6% yield) which was identified as 1:2 adduct of 1,3-dioxolane ribofuranoside derivative whose I.R. spectrum showed a strong absorption for (OH) group at absorption band at 1645 cm^{-1} for olefinic bond (HC=C).

Anal. calc. for $C_{12}H_{18}O_8$ C, 49.65% H, 6.20%

found C, 49.14% H, 6.79%

N.M.R. date:at ppm (δ) 3.7 (A-protons, singlet, ethylene)
4.7 (1-proton, singlet, acetal H)
5-5.7 (1-proton, multiplet, H_3)
4.2 (4-protons, multiplet, H_1,H_4,$2H_3$)
4.7 (2-protons, indistinct doublet, superimposed acetal H, and H_2).
2.45 (1-proton, broad multiplet,OH).
3 (9-protons, singlets, 3 OAc).
2.03, 0.5-1.5 belonged to reagent.

Elution with benzene:methanol 8:2 gave a third fraction (0.23 g.) (13.6%) whose I.R. spectrum was identical with that of the second fraction of 1:2 adduct of 1,3-dioxolane derivative.

Anal. calc. for $C_{10}H_{16}O_7$ C, 48.22% H, 6.45%
found C, 47.38% H, 6.96%

While the last fraction was obtained in (6% yield) whose elemental analysis indicated that it was not a carbohydrate compound.

B: By using 1,3-dioxolane and dry acetone:

A mixture of 1,3-dioxolane (15 ml), dry acetone (2 ml) and D-rival derivative (1) (1 g.) was irradiated for (24) hrs.

A solution of D-ribal derivative (1) (0.5 g.) in acetone (4 ml) was then added in four portions at (24) hrs. intervals and the mixture was further irradiated until there was no change in reaction mixture (144) hrs.

T.L.C. indicated the presence of three components after (72) hrs. which was attributed to the starting material and reagents respectively. The fourth, fifth, and the sixth components were developed after (96), (120), and (136) hrs. respectively.

Excess reagents were removed under reduced pressure and the residue (1,3 g.) was chromatographed on silica gel (50 g.) Elution with benzene gave D-ribal derivative (1) (0.4 g., 26.6% yield), followed by 1:2 adduct of 1,3-dioxolane ribofuranose derivative (0.7 g., 41.6% yield) as a syrup product whose I.R. and N.M.R. spectra were identical with the ones obtained from photolysis in the presence of aqueous acetone.

Elution with benzene:methanol 8:2 afforded a third fraction (0.25 g., 14.8% yield) whose I.R. spectrum was identical with that of the second fraction of 1:2 adduct, while the last fraction was obtained in (5%) yield as a side product.

2. In direct sunlight:

The method of Rosenthal and Elad was followed [1]. A mixture of 1,3-dioxolane (10 ml), dry acetone (2 ml) and D-ribal derivative (1) (0.5 g.) was left in direct sunlight for one day.

A solution of olefinic sugar (1) (0.25 g.) in acetone (3 ml) was then added in seven equal portions at one day intervals and the mixture was left in sunlight for another (8) days.

T.L.C. indicated the presence of three components after (3) days while the fourth and the fifth components were developed after (5) and (10) days respectively. Excess reagent were removed under reduced pressure and the residue (0.6 g.) was chromatographed on a silica gel (40 g.)

Benzene eluted a fraction (0.19 g., 26% yield) which was identified as the starting material. Elution with benzene: methanol 8:2 afforded a second fraction (0.35 g., 41.66% yield) which was identified as 1:2 adduct of 1,3-dioxolane derivative followed by a third fraction (0.12 g., 16.5% yield) which was identified as the deacetylated product of 1:2 adduct of 1,3-dioxolane derivative, while the last fraction was also obtained in (6%) yield as in the previous experiment.

Acid hydrolysis of the 1,3-dioxolane adduct to generate the free aldehyde compound:-

A stirred solution of 2-(2,3,5-tri-O-acetyl- β -D-ribofuranosyl) -1,3-dioxolane (4) (0.25 g.) in acetic acid-water 1:1 (8 ml) was continued for over (24) hrs.

T.L.C. showed a slight change in R_f value and a yellow spot appeared on treatment with alcoholic 2,4-dinitrophenyl hydrazine spray. The product was isolated using chloroform yielding a syrup product (0.1 g.).

I.R. data: Film $\nu_{max.}$ No absorption for (OH) group.
1745 cm^{-1} due to(O=C) of Ac group,
1720 cm^{-1} due to aldehydic group (-CO)
2880 cm^{-1} due to aldehydic proton.

N.M.R. data: at ppm (δ) 8.15 (integrated area was not clear presence of aldehydic H)
5.1 (1-proton, multiplet, H_3)
4.3 (4-protons, doublet, H_1,H_4,$2H_5$)
3.9 (1-proton, triplet, H_2).
2.1 (9-protons, singlet, 3 OAc.)

Base-hydrolysis of 1:2 adduct:-

A solution of 1:2 adduct (2,3) (0.089 g.) in dry ethanol (1 ml) was treated with a solution of sodium ethoxide (2 ml, 0.02 N). The reaction mixture was shaken for (5) hrs. T.L.C. in benzene:methanil 8:2 indicated the presence of two components.

BIO - RAD (Dowex 50 - W - X) resin (H^+) was added to stop the reaction, filtered, evaporated to dryness, yielded a syrup product.

I.R. data: Film $\nu_{max.}$ 3400 cm^{-1} for (OH) groups
1745 cm^{-1} for carbonyl group

N.M.R. data at ppm (δ) 4.7 (1-proton, singlet, acetal)
3.7 (4-protons, multiplet, methylene protons).

REFERENCES

1. I. Rosenthal and D. Elad, Tetrahedron, 23, 3193, (1967).

2. J.S. Jewell and W.A. Szareck, Tetrahedron letters, 43, (1969).

3. K. Matauura et al., Tetrahedron letters, 33, 2869, (1970).

4. S. Hanessian and A.G. Pernet, Chem. Commun., 755 (1971).

5. G. Trummlits and J.G. Moffatt, J. Org. Chem., 38, 1841 (1973).

TREATMENT OF IRAQI WOOL WITH ANTIFELTING AND ANTISHRINKAGE AGENTS

M. K. Sadek and S. A. S. Al-Janabi*

ABSTRACT

Different oxidiation methods to prevent felting and shrinking of wool, were studied, especially copper sulphatehydrogen peroxide and potassium permanganate methods.

In this paper we applied copper sulphate-hydrogen peroxide method.

attempts have been made to find the optimum reaction conditions between wool and hydrogen peroxide in the presence of traces of cooper to perform antifelt and antishrink improvement. Dyeing properties, fastness test, physico-mechanical properties and chemical constitutions were investigated as related to the oxidation

The reactions were carried out at different temperatures and for various length of time and at various pH's.

INTRODUCTION

I: Studies on shrink and felt-resistance as related to copper sulphate-hydrogen peroxide treatment.

There are many factors that could take some part in felting these factors are D.F.E. (Directional Fractional Effect) or scaliness. Some of the major properties that could be affected by felting are: Curliness, Crimpness, and Twist [1].

Physical oxidation and additive prossesses are followed in this paper among other treatments to render wool antifeltable and antishribkable[2]

It has been established that on applying hydrogen peroxide either in acid or alkali media to wool, antifelt and antishrink effects could be obtained [3]. The factors governing these treatments were found to be concentration, pH, temperature and duration of treatment.

(*) Department of Physics, College of Education, Al-Mustansiriyah University, Baghdad - IRAQ.

The reaction between wool and H_2O_2 is powerfully catalysed by heavy metal ion such as copper or nickel [4] . The process was primarily studied by Kantouch and coworkers and it was reported that the treatment of wool for 15 minutes with 0.25 g/L.$CuSO_4$ followed by alkaline hydrogen peroxide treatment (2-4 vol.) rendered wool antishrinkable and antifeltable at 50° C for one hour [5] . The -S-S- bond is readily oxidised in the presence of heavy metals but it is not known whether the oxidation with $CuSO_4$ / H_2O_2 proceed by the same chemical reaction [6]. Graham and Statham investigated the felting of wool in Calcium chloride and zinc sulphate [7]. Nitscchke studied the use of chromium and copper salts [8], Mcphee investigated the reaction of wool with sodium sulphite and Zn^{2+} [9] .

EXPERIMENTAL

Materials and chemicals:

1. Wool :

Iraqi wool (arabi) (100 %) fibers, (50 s), fineness 29.6 u, washed thouroly, scoured then rinsed spinned and woven in fabric, twill 2/2, worsted, wrap 2/24 metric, weft 1/30 metric, ends per inch is 77-78, picks per inch is 73-74, scoured and crabbed weaved in fabric. Copper sulphate (hydrous) and hydrogen peroxide (110 vol.) of pure grade were used.

2. Treatment of wool with copper sulphate and hydrogene peroxide:

Scoured wool is treated in a copper sulphate solution(0.2-2%), adjusted to pH5 (liq.ratio 1:40), four times ranging from 10-60

minutes, with occasional shaking in a thermostatic water bath at temperatures ranging from 40-60°C . The squeezed copper sulphate treated wool is inserted into a new bath containing hydrogene peroxide (1-2 vol.) adjusted to pH4 with sulphuric acid or to pH8 using sodium silicate at temperatures ranging from 10-60 mimutes with occasional agitation.

The treated wool sample was rinsed then treated in an acidified sodium sulphite bath (3g Na_2SO_3 /L, 0.5ml 2N H_2SO_4/L) for 15 minutes at 30°C . Finally the wool was throughly washed with hot then with cold water and finally was air dried .

3. Analytical Methods:

a. Determination of $CuSO_4$ consumption [10] and hydrogene peroxide consumption [11] is calculated from difference in concentration of their solution before and after reaction with wool .

b. Solubility measurements :

Urea-bisulphite solubility [12], and Alkali-solubility [13] are calculated as percentage of the dry weight of the sample .

c. Estimation of total nitrogene in wool by a micro-kjeldahl method [14] .

d. Estimation of sulphure content in wool [15] .

e. Amino acid analysis :

Estimation of tyrosine [16] , tryptophan [17], cystine [18] .

f. Felting and shrinkage test of fabric was estimated [19] .

g. Mechanical measurements :

Tensile strength and elongation [20], Gount number [21] and Twist test 22 .

4. Dyeing of wool :

The following dyestuffs of diffrent classes were used :

No	Name	Class	C.I.	Supplier
1.	Polar brill-RedB	Acid	Acid Red 249	(Ciba - Giegy)
2.	Diamond chrome Red 5G	Chrome	Mordand Red 19	(Bayer)
3.	Neolan Orange G	1:1 Metal complex	Acid orange 62	(Ciba-Giegy)
4.	Remalan Yellow GG	2:1 Metal complex	Acid Yellow 149	(Hoechst)
5.	Cibacron Blue BR	Reactive	Reactive Blue 5	(Ciba-Giegy)

The different classes were applied as mensioned by Bird[2], pH temperature and time are adjusted according to the dyeing process

5. Fastness tests: Fastness tests are reported according to ISO tests as follows: Washing ISO test No. 2 [23] , Fastness to light [24], Fastness to rubbing [25], Fastness to perspiration [26] , Fastness to crabbing [27].

Results And Discussion

In order to accentuate the copper sulphate-hydrogene peroxide improvement, a systematic study of the reaction of wool with copper sulphate , then with hydrogene peroxide and finally with sodium bisulphit was carried out in the limits where wool did not loose its fibrous characteristics. Fig. (1) represent the rates of copper sulphate consumption. It is clear that the rate increased by the increase of temperature and time of reaction .

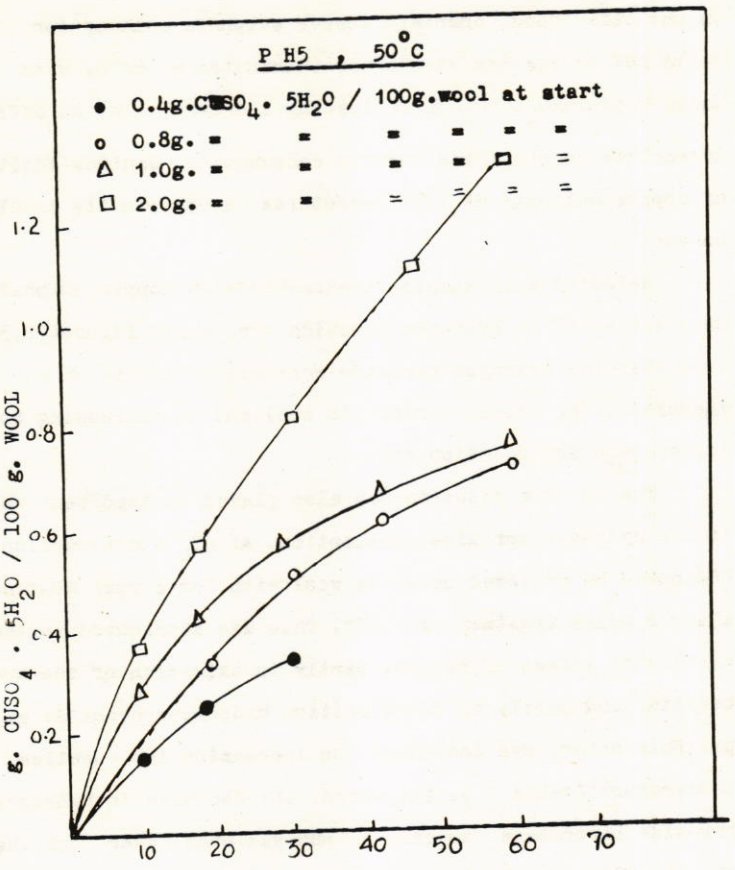

Fig(1): Rate of copper sulphate consumption (g. $CuSO_4 \cdot 5H_2O$/100g.wool).

Complete consumption could be achieved after 10-20 minutes on using relatively low concentrations at 50° C. On the other hand, complete copper sulphate consumption could not be reached even after 60 minutes at 60°C, when using 0.5g $CuSO_4 \cdot 5H_2O$/L indicating a decrease in the affinity of wool to copper after certain consumption. Cautios addition of copper sulphate at low tempretures ascertain its levelling on wool .

Selected wool samples pretreated with copper sulphate were subjected to hydrogen peroxide treatment. Figures(2,3) show that the hydrogen peroxide consumption increased on increasing the copper content in wool and on increasing both temperature and reaction time.

The pH of a solution has also played an important role in the hydrogen peroxide consumption. At pH_4 a consumption of 80% could be achieved on using wool with low copper content after 2 hours treatment at 40°C. This was attributed to the catalystic effect of copper, partly in oxidation of the wool keratin, and partly in decomposition hydrogene peroxide at this pH. This effect was increased on increasing the reaction temperature (table 1). In general the decrease in hydrogen peroxide percentage in case of pH8 was much lower than that of pH4 under identical conditions of temperature, time, and copper content, also the rate is smooth relative to pH4.This can be attributed to the regular decomposition of hydrogen peroxide.

It is clear that pretreatment of wool with copper salts is essential to impart antishrink and antifelt properties to wool.

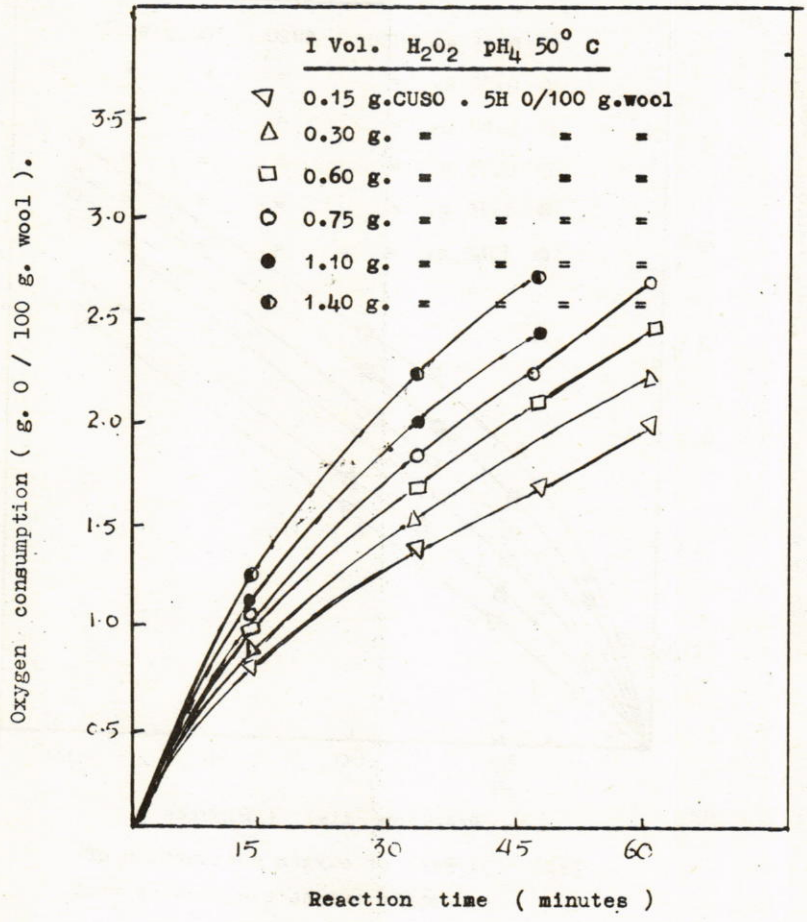

Fig(2): Rate of oxygen consumption of copper sulphate - treated wool

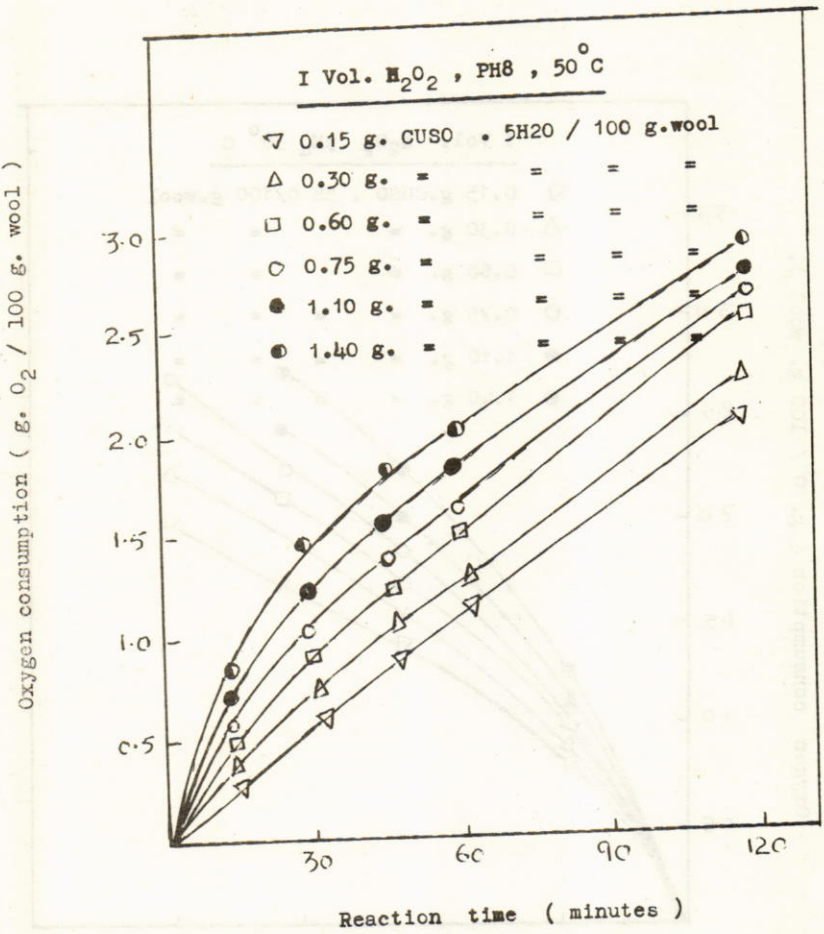

Fig(3): Rate of oxygen consumption of copper sulphate - treated wool.

Table (1)

% Area felt-Shrinkage of wool fabrics treated with copper sulphate followed by hydrogen peroxide at 40°C and 50°C using 1 Vol.H_2O_2 (Area shrinkage of untreated wool = 40%).

$CuSO_4 \cdot 5H_2O$ consumption g/100g.wool	pH	40°C		50°C	
		½ h.	1h.	½h.	1h.
0	4	46	50	52	60
	8	42	45	44	48
0.15	4	40	-	38	38
	8	38	35	36	35
0.30	4	10	14	8	14
	8	6	6	4	4
0.75	4	10	16	10	19
	8	6	-	6	8
1.4	4	14	20	20	22
	8	12	-	12	-

This may be due to increased attack of peroxide on whole material and not only on the surface. On the other hand, treatment of wool with $CuSO_4$ only, do not change the area shrinkage.

In general, wool samples which has consumed 0.3g $CuSO_4 \cdot 5H_2O$ and then treated with 1 vol. H_2O_2 at pH8, showed improvement in their antishrink properties. This can be explained by the effective role of copper in restricting the peroxide oxidation to certain points on the scales because of marginal absorbance of Cu on these points. Thus the gradual increasing effect of copper sulphate consumption related to area shrinkage could be put in the order 0.3 0.75 0.15. It is worthy to mention that increased amounts of copper salts highly affected the white colour of wool, probably due to the precipitation of CuS on the surface and inside the fiber .

The samples were subjected to an acid treatment with 3g/L. Na_2SO_3 in H_2SO_4 for 15 minutes at 30°C to remove the greenish-brown colour and the residual O_2 from the wool.

Dyeing properties:

From table (2) we clarified the influence of these antifelt treatments on the dyeing properties of wool. It has been found that these treatments increased to some extent the wool affinity and exhausion towords the different classes of dyestuffs, with the same levelling effect.

It gave relatively dull shades compared with those of untreated wool, it increased washing fastness of acid dyes, due to an ion effect which increase the dye-fixation on wool.

The influence of the antifelt treatments on chemical constitution shows that sulphure and cystine contents decreased due to the oxidation reaction at the optimum conditions table(3).

Table (2)

Fastness tests of acid dyes on copper sulphate - hydrogen peroxide treated wool

Dyestuff Used	Sample	Washing 2			Preparation			Potting	Rubbing				Light
		Alteration	Staining		Alteration	Staining		Alteration	Staining		Dry	Wet	
			W*	C*		W	C		W	C			
Acid dyes:													
Polar Bill Red B	Untreated	3	2	2-3	3	2	1-2	2	2	3	3	2-3	3
Polar brill Red B	Treated	3-4	2	2-3	3	2-3	2	2	3	3-4	3	3	4-5
Chrome dyes:													
Diamond Chrome Red	Untreated	4-5	5	4-5	4-5	4-5	4-5	3-4	4-5	4-5	5	5	6-7
	Treated	4-5	5	5	5	4-5	5	4	4-5	4-5	5	5	7
1:1 Metal Complex:-													
Nealan Orange G	Untreated	3-4	4	4	3	4	4	4	4	3	4	4	6
	Treated	3-4	5	4	4	4-5	4	4-5	4-5	3	4-5	4	6-7
2:1 Metal Complex:-													
Remalan Yellow GG	Untreated	3-4	4-5	5	4	3-4	3-4	3-4	4-5	4	4	4	5
	Treated	4	5	4-5	4	4	3-4	4	5	5	4	4	6
Reactive:-													
Cibacrolan Brill blue RR	Untreated	4	4-5	4-5	4	5	4	4-5	3-4	4-5	4-5	4	5-6
	Treated	4	5	4-5	4	5	4	4	4	4	4	4	6

W* = Wool
C* = Cotton

Table (3)

Amino acid characteristics and solubility of treated wool

Treatment	O.C g O_2/100 g.wool	Cystine %	Tyrosin %	Typto-phan %	N%	S%	Solubility % Alka. line	Solubility % U.B.*
Untreated	0	12.30	4.10	0.72	16.40	3.80	14.30	41.80
(0.1g.$CuSO_4 \cdot 5H_2O$ 1 Vol. H_2O_2)½ h.	0.8	12.00	4.00	0.67	16.30	3.47	21.40	48.10
(0.6g.$CuSO_4 \cdot 5H_2O$ 2 Vol. H_2O_2)2h.	4.2	8.80	3.60	0.62	15.40	3.20	23.20	56.70
(0.7g.$CuSO_4 \cdot 5H_2O$ 2 Vol. H_2O_2) 1h.	3.7	9.00	3.60	0.63	14.50	3.30	20.40	53.0
(0.7g.$CuSO_4 \cdot 5H_2O$ 2 Vol. H_2O_2)3h	-	7.80	2.40	0.42	-	3.12	20.40	53.70

*U.B. = Urea - bisulphite

A bleaching operation using 2 vol. H_2O_2 for 2 hrs., gave the same level of sulphure and cystine contents. This confirm the idea that copper acts as a catalyst for oxidation. Nitrogen contents of wool slightly decrease by the treatment indicating that this operation is not hrmful to dipeptide and free amino groups . The decrease in the sulphure and cystine contents is reflected on the solubility of wool in alkali and urea-bisulphite solution. This may also confirm the breakdown of the cystine bonds leading to formation of other sulphure containing amino acids as a result of oxidation.

Table (4)

Tensile strength, elongation and count number.

Sample	T.S.*		Elongation%		Count Number	
	Wf*	Wp*	Wf	Wp	Wf	Wp
Untreated	21.1	14.2	2/40.6	2/39.9	26	2/32.9
Treated $CuSO_4.H_2O_2$	20.7	13.8	2/41.4	2/45.2	26.2	2/32.7
Bleaching treatment with H_2O_2	20.9	14.0	2/41.1	2/41.1	-	-
Treated $CuSO_4.H_2O_2$ and bleached	19.9	14.0	2/48.6	2/41.9	-	-
Copper sulphate only	21.0	14.2	2/40.8	2/40.1	-	-

*Wp = Warp

*Wf = Weft

*T.S.= Tensile strength. K. gm/meter.

Count Number : (metric) = length of yarn in meter/weight in gm.

Typosine and tryptophan contents of treated wool showed less effect as compared with the bleached one.

Table (4) shows that mechanical properties such as tensile strength, count number, elongation increased in both weft and wrap direction. Microscopic investigation of treated wool shows

that the wool scales had lost their serrated edges, also its abrasion and pilling resistance had improved, copper ions improved bacteria and moth-proofing properties. Also the handle and colour of the treated wool was not greatly effected .

REFERENCES

1. P. Alexander, R.F. Hudson and C. Earland, "Wool, its chemistry and physics " 2nd Edit.,Chapman and Hall Ltd.,London,Ch.8, 281 (1963).
2. C.L.Bird," The theory and practice of wool deying"3rd. Ed., Dean house, Piccadilly, Bradford, Yorkshire, (1965).
3. P. Alexander, D. Carter and C. Earland, J. Soc. Dye. Col.,67, 23, (1951).
4. P. Gunliffe, J.L.Sharp and F.Ashworth, British patent 614,966, (1948).
5. A.Kantouch and F. Peter, Text. Mfr., 91, 298,(1965);Proc.3rd. Inter. Wool Text. Res. Conf., Paris(1965)Sec.III; Kolor, Ert., 8, 302 (1966).
6. M.A. Andrews, J. Biol. Chem., 102, 253, (1933).
7. D.R.Graham and K.W. Statham, Text. Res.J.,30,151 (1960).
8. G.Nitschke, Melliand Textilber, 42, 818 (1961).
9. T.R.McPhee, Text.Res. J.,35, 382 (1965).
10. A.I.Vogel, "Quantitive inorganic analysis,Theory and practice" Longmans, Green and Co., London, 418 (1948).
11. Ditto, 354 (1948).

12. J.H. Dusenburg, J.Text. Instituted, 51, T 758 (1960).

13. L.Leuvean, M.Caillet and N. Demonanart, Bull.Inst.Text.France, 90, 7, (1960).

14. J.E.Varner, W. A. Bullen, S. Vankcko and R.C. Burrell, Anal.Chem., 25, 1528 (1953) .

15. G.F. Smith, Anal. Chem. Acta, 8, 397 (1953).

16. G. Blankeberg and H. Zahn, Textil-praxis, 16, 228 (1961).

17. J. H. Bradbury, Text. Res. J., 31, 735 (1961); J. Text.Inst.,51, T 1226 (1960).

18. K. Sinohara, J.Bio. Chem.,109, 665 (1935).

19. Technical Information, B.A.S.F. Nov.(1969) Tx. 139 e.

20. ASTM Designation, D 1682- 59 T (1962).

21. Ditto, B 1907 - 61 T (1962).

22. Ditto, D 1422 - 59 T (1962).

23. Draft proposal for ISO recommendation. (B.S. 2684).(1961).

24. I.S.O. recommendation R. 105, Part II,(B.S.1006) (1961).

25. Ditto, Part 18, (B.S. 2677) (1961).

26. Draft proposal for ISO Recommendation.

27. I.S.O. Recommendation R 105, Part 16, (B.S. 2675) (1961).

SPECIFIC ADDITIVES FOR EXTENDING THE THICKENING TIME OF THE CEMENT USED IN OIL CASINGS

A.F. Roomaya *, I.K. Al-Haddad and A.K. Wahid

ABSTRACT

A tracer technique was employed for studying the efficiency of mixing quebracho extract** solution with cement. Neutron irradiation samples of sodium acetate were used in the first experiment and of sodium oxalate in the second. It was found that the irradiated anhydrous sodium acetate absorbs moisture and the salt adhered to the irradiated container and was removed with difficulty. However, the use of sodium oxalate tagged with Na-24 as an indicator was a success. When the solution was allowed to mix with cement clinker (0.1-0.2%) the rate of change of activity varied by 1.5 to 12% Background contributions were negligible.

INTRODUCTION

Radioisotopes are ideal tools for studying mixing uniformities of liquids, colloids, slurries, gases, and dry solids. A small amount of a radioactive tracer can be added to bath of material and attainment of a uniform count rate in repeat samples indicates uniform mixing.

The use of a gamma-emitting tracer, with a count rate meter and a strip-chart recorded permits following the course of the mixing process without the necessity for sampled analysis.

---

* Department of Chemistry, College of Science, Al-Mustansiriyah University, Baghdad, IRAQ.
Al-Mustansiriyah Journal of Science, Vol. 5 No. 1 (1980).

** Quebracho extract is a fine red power made from water extract of the bark of a South American tree. It contains alkaloids and considerable quantity of tannin.

A detector may be placed external to the mixer or may even be dipped in the fluid can provide a continuous measurement of the mixing process. If samples are taken, they can readily be analysed with a standard well counter. Hull et. al [1] described a mixing experiment with oil using Zr-95 as a tracer and King [2] determined the efficiency of mixing in an alkylation process using Rb-86.

In this paper a mixing study of a cement (liquid and solid phases) was carried out using a solution tagged with Na-24. A sodium iodide scintillation detector was installed externally and connected to a rate meter and recorder. The record of activity versus time demonstrated the degree of uniformity of the mixing process.

EXPERIMENTAL

As a preliminary experiment, one gram of Quebracho was introduced into a polyethlene vial and enclosed in an Al-container. The container was neutron irradiated inside the central vertical channel of the reactor for ten minutes at a flux of 1.5×10^{13} n/cm^2/sec. The sample was left to cool for nearly 24 hours. By the end of this period the activity due to Na-24 was measured and found to be insufficient for using quebracho extract itself as a tracer. Therefore, anhydrous sodium acetate (3.0g) was irradiated at a flux of 1.5×10^{13} n/cm^2/sec for ten minutes. The clinker feed was found by the end of the experiment to be very humpy and this resulted in a non-uniform flow rate.

The experiment was repeated using sodium oxalate as a labelling compound; (4.0g) of this substance was irradiated in the same manner described earlier for ten minutes at the same flux and the resulting activity of Na-24 was nearly 50 mCi soon after the sample was taken from the reactor.

After irradiation the Al-container was placed in lead shielding and transferred to the cement plant where the experiment was performed. The sample was poured into the dissolving tank of the Quebracho extract and mixed thouroughly. The liquid was allowed to flow into the cement clinker which was fed at a rate of 11 tons/hour; the activity was monitered by an electronic arrangement shown schematically in Fig.(1.)

The background activity was minimized by serreunding the detector sides with lead shielding. Forced ventillation was used in order to keep the detector working at normal temperature. Table(1)gives the relevant experimental conditions for each experiment.

RESULTS AND DISCUSSION

The results obtained from the first and second experiments are listed in tables (2) and (3) respectively. The count rate of sodium acetate mixed with Quebracho solutions is listed in Table 2 for 21 samples. The background was 1600 counts/min. The count rate from sodium oxalate mixed with Quebracho solution is listed in Table(3). The background contribution was 900 counts/min. It is clear from this data that uniform mixing has been achieved during the second run. While the mixing was non-uniform in the first

Inspection of Fig. 2 shows that the spread around the mean was from 1.5% to 12%. Allowing for inherent fluctuations due to counting statistics as well as the decay of Na-24, the results indicate that the mixing was satisfactory during the experiment under these conditions.

The sodium oxalate was added to the Quebracho extract tank (170 litres of solution, two parts of Quebracho to 5 parts of water) at 13:00 hours. The Quebracho extract solution was fed

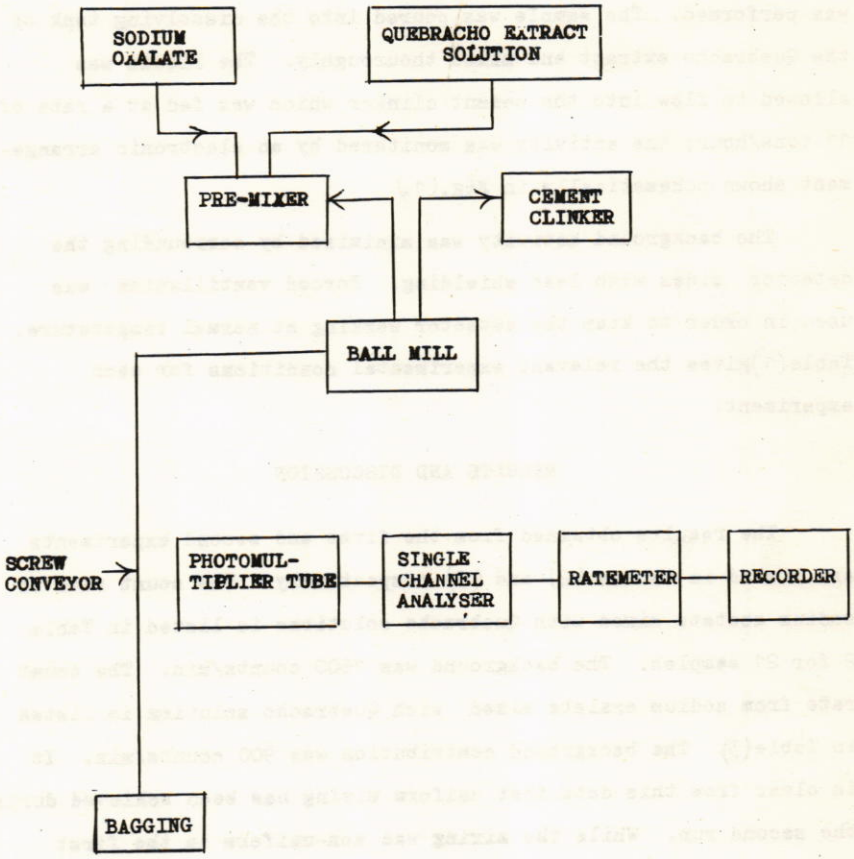

FIG. 1

FLOW SHEET FOR CEMENT MIXING WITH QUEBRACHO SOLUTION

TABLE 1

	Type of comp.	Quantity used	Flow rate	24-Na Acitivity	Irradiation time
First experiment	Sodium acetate anhydrous	3.0 gm	Humpy	30 Ci	10 minutes
Second experiment	Sodium oxalate	4.0 gm	Uniform	50 Ci	10 minutes

TABLE 2

Sample No.	Count/min.
1	35000
2	29500
3	30900
4	29000
5	29000
6	35500
7	40000
8	35500
9	34200
10	40100
11	40600
12	34200
13	41900
14	47900
15	46600
16	46800
17	71100
18	67800
19	56600
20	44800
21	30500

TABLE 3

Time (Hours)	Counts/min
13.16	1000
13.31	1100
13.38	3050
13.46	12000
13.53	43000
13.56	51000
14.06	84000
14.26	120000
14.50	2250000
14.58	230000
15.06	230000
15.10	228000
15.15	235000
15.18	230000
15.21	230000
15.27	235000
15.33	233000
16.00	235000
16.05	235000
16.11	235000
16.16	150000
16.24	100000
16.27	60000

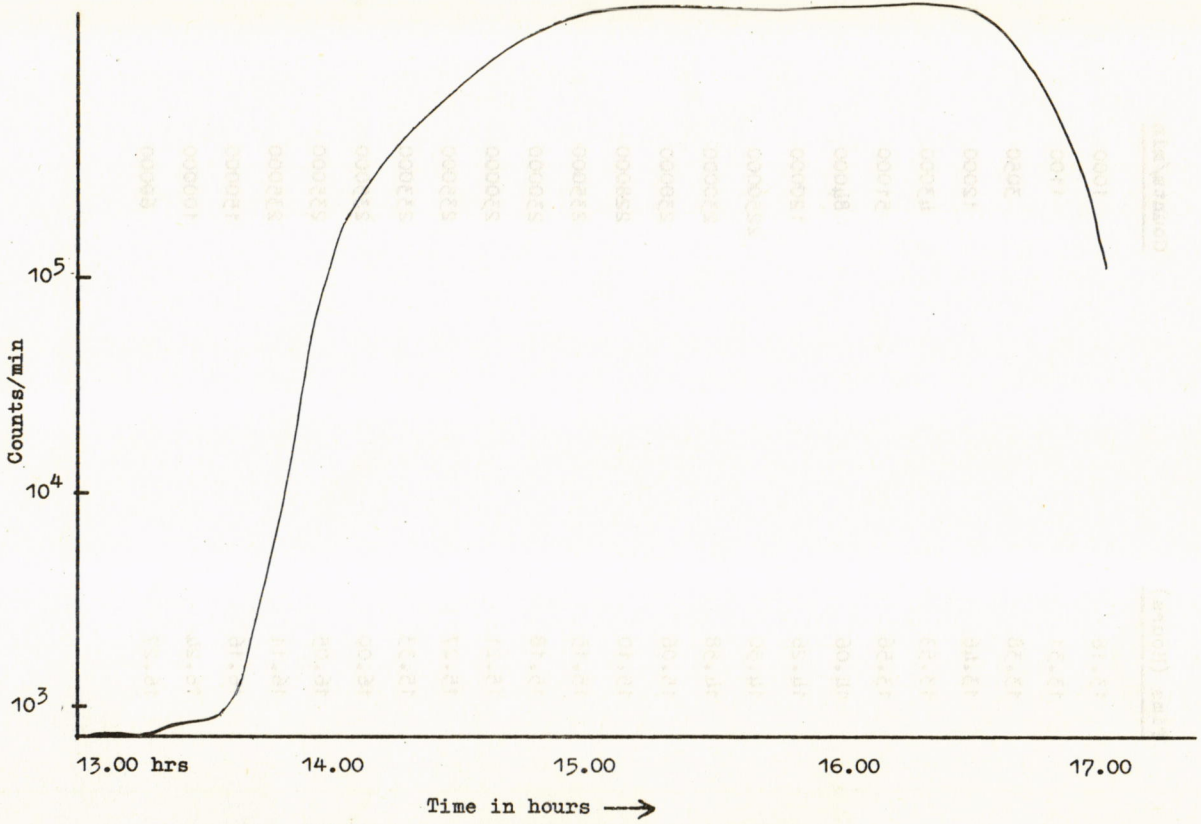

Fig. (2) Variation of counting rate with time

into the clinker at 13:10 hours, but the Na-24 did not reach the clinker until 13 20-hours and at 13.31 hours the radioactivity reached the NaI detector at the screw conveyor, showing a ball mill residence time of 11 minutes. A steady state of radioactivity was reached in 87 minutes (14:58 hours) as shown in Fig.(2). There was 6-7 tons of cement in the ball mill. For 38 minutes after the steady state was reached (14:58) to 15:36 hours) the fluctuations (decay corrected) were about 1.5% and this continued to the remaining time (at about 16:10 hours). The maximum deviation from the mean decay corrected) was 12%.

The radioactive decay from 14.58 to 16:10 hours was about 5.4% of the radioactivity at 14.58 hours. Background varied from 955 cpm at 13:00 hours to 1153 cpm at 11:53 hours before the radioactivity reached the detector.

The activities required for a flow experiment with external recording depend on a number of factors such as the self-absorption of the radiation in the labelled material, the solid angle covered and the detection efficiency of the system. The spread from uniformity that has been observed may be due to such factors as well as counting statistics.

REFERENCES

1. D.E. Hull et al, Nucleonics, 14, 51, (1956).
2. W.H. King, Ind. Eng. Chem. 50, 201 (1958).

ACKNOWLEDGEMENTS

We wish to thank Mr. G. E. Smith, Technical Assistance expert, LAEA, for many valuable discussions. Thanks are also due to Mr. Z. Kosina, Mr. W. Mutammara, and others at the Oil Reasearch Institute for their cooperation and assistance.

PHYSICAL PROSPERTY GUIDE FOR ROCKS FROM IRAQ

M. Mashkour* and M. Berifkani*

ABSTRACT

The properties of rocks of which most use is made in geophysical prospecting are density, magnetic susceptibility, electrical resistivity, compressional semismic velocity and to a less extent shear seismic velocity.

The present reference guide which is the first of its kind is intended to determine physical properties of rocks from Iraq. Laboratory measurements were conducted on cores of various sizes drilled from samples belongs to 27 types of rock, mainly limestones and marbles. Total of 200 cores were prepared and used in the various physical tests.

INTRODUCTION

It is necessary to have some knowledge of the phycisal properties of rocks for estimating the strength of geophysical indications that different geological features, rock masses ore bodies etc. can yield, as well as for assessing in advance whether and if no within what limits, a projected geophysical survey in an area is likely, to serve its purpose. The physical properties of naturally occurring rocks and minerals vary within wide limits and for the purpose of any

* Department of Geology, College of Science, Al-Mustansiriyah University, Baghdad, IRAQ.

Al-Mustansiriyah Journal of Science, Vol. 5, No. 1 (1980).

particular survey, they should be determined as far as possible on a large number of rock samples from the relevant area. The present reference guide is not intended to be a substitute for such determinations.

The properties are also highly dependent on such factors as temperature and pressure, but this aspect is not considered here. The values mentioned are for room temperature ane atmospheric pressure, but in some work it may be necessary to supplement them by a knowledge of the effect of temperature (e.g. in permafrost regions) or by a knowledge of the effect of pressure (e.g. in deep-well logging).

The properties of rocks are highly dependent on various factors such as texture (e.g. grain size, schistosity, bandedness etc.), properties of the minerals constituting the rock and their mode of distribution, the volume of pore space and the tortuosily of that space and the amount, the physical proportions and the state of the water in the pores. Consequently, even when samples of rocks come from the same petrographic and geologic unit their properties may vary considerably. Many (Laws) or mathmatical expressions describing the dependence of the physical properties of rocks and minerals on one or more of the above mentioned factors have been suggested. Some of these (e.g. that for density) can be deduced from theoretical considerations but usually it is necessary to base them on empirical material. In the latter case an expression derived from measurements in samples in one area or for rocks of one geological age may not be valied for samples in another area or for rocks of some other age.

Physical properties of rocks (Definitions, Units, Variations and geophysical implications)

I. Density: A measure of ponderability (heaviness) of a body, being mass per unit volume. Expressed usually as gramme per cubic centimetre, denoted by the greek letter (σ) (Sigma).

The gravitational attraction of a homogeneous body is directly proportional to the difference between its density and the density of the surrounding rock.

The density of sedimentary (and some igneous) rocks correlate in a general sort of way with the geologic age. Older rocks usually have a greater density than younger ones, west [1].

Most rocks, especially sedimentary ones but also many igneous rocks, have appreciable porosity and their density in situ depends on the extent to which the pores are filled with water, It is therefore advisable to determine a dry and a saturation density of a sample to obtain the possible limiting densities **in situ.**

II. Magnetic Susceptibility: Magnetic susceptibility is, like density, a physical property of the materials in bulk. Susceptibility may be described as the ability of a materials to take an induced magnetism, that is, to become temporarily magnetized when placed in an external magnetic field. For a homogeneous isotropic body the ratio of the induced intensity of magnetization to the external magnetizing force inducing it, denoted by the greek letter (κ Kappa). Although (κ) is a dimensionless number, its magnitude depends on whether the intensity of magnetization and the causetive fórce are measured in the same units

or not. The former is the case for the Systeme Internationale (SI) the latter for the electromagnetic centimetre - gramme - second (e.m.c.g.s) system in which the intensity of magnetization is measured in obsolute ampere per centimeter but the external magnetising force in units of ($\frac{1}{4\pi}$ absolute ampere per centimeter). The absolute ampere is equal to 10 (ordinary) ampere.

Consequently, the magnitude of (χ) expressed in (SI) is (4π) times that expressed in e.m.c.g.s system. Converesly the magnitude of (χ) expressed in e.m.c.g.s. is ($\frac{1}{4\pi}$) times that expressed in (SI). Most earth materials have positive (χ), these are known as para magnetic, few substances such as salt and Anhydrite, have negative (χ) and are described as diamagnetic.

The low-field magnetic susceptibility of rocks depends almost entirely upon their content of magnetite, titanomagnetite, ilmenite and pyrehotite, ilmenite and pyrehotite, but rocks can have small but appreciable positive or negative susceptibilities even without these minerals. The (χ) of pure magnetite is a fairly definite, so that a relation between the (χ) of a rock sample and its magnetite content can be experimentally determined. An expression derived by Balsley and Buddington [2] from measurements on the metamorphic samples from the Adirondack area (U.S.A.) may be written as

$$\chi = 0.0326 \sqrt[3]{v^4} \qquad \text{(SI)} \ldots\ldots\ldots\ldots (1)$$

Where (V) is the volume percent Fe_3O_4.

Mooney and Bleifuss [3] have derived the following relation for Fe_3O_4 content up to 20 percent

$$\chi = 0.0361 \ v^{1.01} \qquad \text{(SI)} \ldots\ldots\ldots\ldots (2)$$

Such formulas seem to give the susceptibility of magnetite-bearing rocks to within a factor of 2-5 for small magnetite contents and within some 10-20 percent for high magnetite contents.

III. Electric resistivity:- For homogeneous, isotropic body carrying an electric current, the ratio of the electric intensity (Voltage per unit distance) at any point within the body to the current across area perperdicular to the electric intensity) at that point is the electric resistivity. Expressed usually as ohm - m, or Ω m (that is ohm times metre), and denoted by the greek letter (ρ) (rho). The electric resistivity is the one of the most variable of all the physical properties of rocks. The variations can be primarily classed in three categories: (1) the scatter of observations on one and the same sample. (2) the variations among samples of the same rock type and (3) the variations among different rock types. These variations overlap to a considerable degree and often make it difficult to assign resistivity values or even ranges of values to single samples and rock types.

The causes of variability are numerous. The conductivities and the mode of distribution of the minerals in a rock sample have a dominating effect on the resistivity is also affected by the grain size. The coarser the grain size in a rock the higher is the resistivity, other things being equal.

The resistivity (ρ) of porous water-bearing rocks (free of clay minerals) follows Archies Law, Killer and Frischknecht

$$\rho = \frac{\rho_o}{f^m z^n} \qquad \ldots\ldots\ldots\ldots (3)$$

Where (ρ_o) is the resistivity of the water filling the pores, (f) is the porosity (volume fraction pores), (S) is the fraction of pore space filled by the water and (n), (m) are certain parameters. The value of (n) is usually close to (2.0) if more than about 30 % pore space is water-filled but can be much greater for lesser water contents.

The value of (m) depends upon the degree of cementation or, as this is often well correlated with geologic age, upon the geologic age of the rock. It varies from about 1.3 for Loose, Tertiary sediments to about 1.95 for well cemented paleozoic ones, but can be outside this range for individual formations. Compact cretaceous and jurrasic sandstone often have (m) close to or slightly exceeding (2.0).

Highly porous rocks have an m-value of the same order as loose to moderately cemented sediments.

Layered rocks such as shales, gneisses, phyllites etc. and banded rocks often exhibits anisotropy of resistivity. The resistivity parallel to the layers is less than that perpendicular to the layers.

The electric resistivity of rocks has been very thoroughly treated by Park homenke [5]

IV. Seismic compressional and shear wave velocities:- Distance travered by compressional waves deonted as (P) or shear waves denoted as (S) in unit time. Expressed in (SI) as metre per second (m/s).

During passage of a compressional wave each particle of the medium oscillates parallel to the direction of propagation of the wave. Shear waves, in which the particles Oscillate

perperdicular to the direction of propagation, are Seldom availd of in applied semismology.

The energy of an explosive underground shot goes predominantly in compressional waves. The partition of energy of compressional waves, incident on an interface between two media, into a reflected and a refracted part is governed by the difference in the acoustic impedences of the media. The compressional acoustic impedence (expressed in (SI) as Kilogramme per sq. metre per second) of a medium is the product of the longitudinal velocity and the density of the medium is the product of the longitudinal velocity and the density of the medium.

Although variations of seismic velocities within and between different rock types show a certain overlap it is found that in restricted areas, different geological formations and rock types often have characteristic seismic velocities. This is particularly true of sedimentary formations, in which the velocity appears furthermore to be correlated with the depth of burial and geologic age.

According to Faust [6], the velocity of compressional waves in shales and sands can be described by the relation

$$V_p = 46.5 \sqrt[6]{ZT} \quad \text{m/s} \quad \ldots\ldots\ldots (4)$$

where (Z) is the depth in metres and (T) is the age in millions of years.

Methods of Laboratory Measurements on Samples

Meaningful determinati[on] the physical properties of samples of rocks that describes the relevant property can only be made on homogeneous or quasi-homogeneous samples. A quasi-homogeneous sample is one in which the inhomogenities are more

or less randomly distributed and size of which is large compared to the size of the largest inhomogeneity. If the inhomogenities are systematically distributed (e.g. parallel layers of differing composition), meaningful determinations of the magnetic, electric and seismic properties can still be made on many samples. However, they do not lead to a single parameter value but to a set of up to six values unique to the particular sample. This set (reducible) to three or, in some cases, two) is called the tensor of the sample.

Although the collected surface rock block samples (see Fig. 1) quesi-homogeneous, but tests were made on cores drilled from three direction of each block (See Fig. 2) so that every inhomogencity will be represented in the test and hence a better representative physical property value (for the particular rock type) will be obtained.

Great variety of methods of measuring the physical properties of rock samples exist, some of which are highly elaborate. The methods described here are of the simpler type and chosen so that the desired measurements can be made with a minimum of apparatus.

I. Density - The clamic method of determination was applied. This involves the measurement of weight (w) and volume (v) of a rock piece, A rock core of (½" Dia. by 1" length) was weighted by a very sensitive balance read to the hundredths of the grames. The volume was measured by totally immersing the rock core in a finely graduated cylinder. The volume of the rock core will be the equivalent volume of the displaced water in the cylinder.

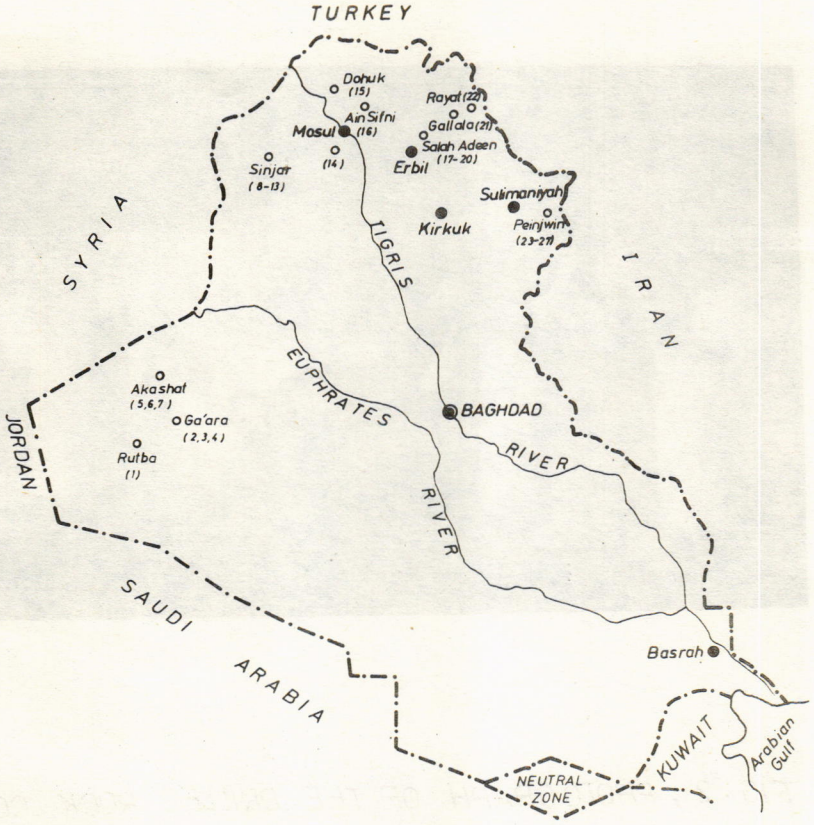

Fig. 1 .Location map of the collected rock block samples

FIG. 2, PHOTOGRAPH OF THE DRILLED ROCK CORES.

Two types of densities were measured. The dry and wet (section 2). For the dry density, the rock core was dryed in the oven at 105° for 24 hours. While in the saturated density measurements the saturation was made in the water for 24 hours, one test for each density was made. Results of the test are given in table.

II. Magnetic Susceptibility :- Two laboratory methods were tried. Firstly the MS-3 magnetic susceptibility bridge. Here the readings depends on the difference in the tone before and after inserting the tested specimen in the bridge. 1" dia by 4" length cores were used. Since most of the tested rock of a very low in magnetic susceptibility hence it was found hardly to detect any difference in the tone and therefore any readings. For that another magnetic susceptibility equipment was used. i.e. the Kappameter here the reading can be noted by any deflection in the needle when the rocks are tested. Measurements were made on the rock blocks themselves. Some of 10-15 readings were taken. The values in (SI) was then converted to e.m.c.g.s system (see sect. 2). Some of the tested rocks have given very low value of magnetic susceptibility other not. For results see the table.

III. Electric resistivity - In one commonly used arrangement a sample in the form of a rectangular prism or a drill core with flat ends is clamped between two metal plates connected to a current source. Let (I) ampere be the current passing through the circuit and ($\triangle$ V) the voltage across the probes placed on the sample, along a line perpendicular to the end faces through which the current enters and leaves the sample Then the resistivity is given by

$$\rho = \frac{\triangle V}{I} \quad \frac{S}{L} \qquad \ldots\ldots\ldots\ldots (5)$$

Table of Physical Properties of rocks from Iraq

No.	Rock Name	Formation	Dry Density (σ) gm/cm^3	Saturated density (σ) gm/cm^3	Magnetic susceptibility (χ) c.g.s.	Electrical resistivity (wetted rock) (ρ) Ω.m.	Compressional wave velocity (Vp) m/sec.	Shear wave velocity
1.	Sandstone	Rutba	2.518	2.523	0	142.24	6785	4523
2.	Limestone	Mullussa	2.520	2.720	0	2.928	4773	3068
3.	Sandstone	Gaara	2.296	-	0	-	-	-
4.	Limestone	Dammam	2.430	2.525	0	13.45-20.5	3294	2812
5.	Limestone	Um-El-Radhuma	2.406	2.496	0	5.97-14.43	5016	3173
6.	Limestone	Tayrat	2.487	2.578	0	10.338	2160	1912
7.	Limestone	M'sad	2.027	2.305	0	1.01	3446	2278
8.	Marly Limestone	Shiranish	2.519	2.606	$(6-27)\times 10^{-6}$	16.44-28.5	5258	2867
9.	Limestone	Shiranish	2.367	2.525	0	2.34	5403	3396

No.	Rock Name	Formation	Dry Density (σ) gm/cm^3	Saturated Density (σ) gm/cm^3	Magnetic Susceptibility (χ) c.g.s.	Electrical Resistivity (Wetted rock) (ρ) Ωm.	Compressional Wave velocity (Vp) m/sec	Shear wave velocity (Vs) m/sec
10.	Limestone	Sinjar	2.615	2.605	0	91.4.507.5	3770	2436
11.	Limestone	Jadala	2.208	2.367	0	1.22-2.33	4038	2558
12.	Limestone	Serikagni	2.410	2.547	0	3.5-5.0	4720	2836
13.	Limestone	Jeribe	2.624	2.650	$(0-15)\times10^{-6}$	118.9	5813	3543
14.	Gypsum	Upper fars	2.508	3.120	Negetive Value (just below zero)	376.4-683.3	2830	1934
15.	Sandstone	Gercus	2.208	2.410	$(3-21)\times10^{-6}$	2.12	-	-
16.	Limestone	Lower Fars	2.442	2.526	$(5-10)\times10^{-6}$	9.9-16.7	4285	2369
17.	Limestone	Pilaspi	2.578	2.707	0	3.43	4830	3180
18.	Sandstone	Upper Fars	-	-	$(30-120)\times10^{-6}$	-	-	-
19.	Dolomitized Limestone	Pilaspi	2.700	2.708	$(0-3)\times10^{-6}$	568.3	6038	3394

No.	Rock Name	Formation	Dry Density (σ) gm/cm^3	Saturated Density (σ) gm/cm^3	Magnetic susceptibility (χ) c.g.s.	Electrical Resistivity (Wetted rock) (ρ) Ωm.	Compressional Wave velocity (Vp) m/sec	Shear wave velocity (Vs) m/sec
20.	Perish Marble	Penjwin group	2.677	2.690	$(0-10)\times10^{-6}$	141.7	5770	3753
21.	Gallala marble	Walsh	2.730	2.739	$(3-9)\times10^{-6}$	1454.42	6508	3518
22.	Rayat marble	Naepurdan	2.768	2.769	0	$> 0.51\times10^{4}$	6388	3549
23.	Kani Kwish gray marble	Penjwin group	2.760	2.764	$(18-82)\times10^{-6}$	$> 0.46\times10^{4}$	6085	3054
24.	Kani Kwish gray marble	Penjwin group	2.726	2.729	$(1.5-15)\times10^{-6}$	$> 0.34\times10^{4}$	6632	3714
25.	Qulaka marble	Penjwin group	2.653	2.657	$(0-27)\times10^{-6}$	522.5	5323	2907
26.	Merga-Seed Marble	Penjwin group	2.444	2.446	$(0-4.5)\times10^{-6}$	2289.5	666	3668
27.	Qarachmach marble	Penjwin group	2.686	2.693	$(9-39)\times10^{-6}$	$> 0.417\times10^{-4}$	6536	3856

where (S) the area (m^2) of the end faces and (L) metre is the distance between the probes. The distance (L) must be large in comparison to the inhomogeneities in the sample.

In the experiment the core resistivity apparatus utilizes the two electrode method described above was used.

Core samples lengths at least four times the diameters (¾" Dia. by 3½" length) were used, the ends faces were made smoothed, flat, and parallel to insure good contact with the electrodes.

The cores were saturated by plating in salt solution of unknown concentration for 24 hours. The cores then screwed between platens, which are themselves covered by saturated chamois, The value of resistance ($\frac{\Delta V}{I}$) in the equation (5) was read directly from the instruments. Three cores for each type of rock were tested. Test results are given in the table.

IV. Compressional and Shear Wave Velocities:- Laboratory determinations of the velocity of sound in rock samples are usually carried out on drillcores. It may be thought that the same determination could be easily carried out by striking a hammer blow at one end of the core and measuring the time that the impulse takes to appear at the far end. However, there are several difficulties in the experiment. Even in cores of some length (say 25-50 cm) the travel time is only some tens of microseconds. The sensing device at the far end must make an intimate contact with the sample as the time delay introduced by a poor contact can be of the same order of magnitude as the travel time along the core.

The instant of blow must be accurately defined. In samples of loose material (clay, sand, moraine etc.) the absorption of elastic energy is appreciable and the impulse arriving at the sensing device may be too weak to be determined. For these reasons the apparently simple method above is often not accurate or even feasible. The proper determination of the velocity of sound in rock samples requires more refined apparatus. Therefore seismic analyzer which provides direct digital readout of ultrasonic delay times between (0) and 999.9 micro seconds with a resolution of 0.10 micro seconds was used. Both compression and shear wave delay time (velocity) measurement can be made with this equipment. The equipment is fitted with two pairs of dual-mode combination compressional (P) and shear (S) waves transducers, operating at 300 KHz and 1 MHz. Throughout the work, the 300 Khz was used both as exciters and receivers for (P) & (S) seismic waves velocity measurements.

The wave velocity is not determined directly but is calculated from the time taken by a pulse to travel a measured distance. This ultra sonic pulse is obtained by applying a rapid change of potential from a transmitter exciter to a piezoelectric crystal transduced emitting vibrations at its fundemental frequency.

With the equipment used in our experiment the original signal from the receiver is displaced on oscilloscope screen.

In using the ultrasonic material tester, there are some factor which govern the accuracy of the measurements. There are as following:

A) The effect of Specimen and condition - Although the specimen does not need to be regular in shape, but it must have prefectly parallel ends.

B) Coupling of the transducers to the specimen - In order to facilitate good contact between transducers and the rock specimens, ordinary grease must be used as a coupling agent. This allowed sufficient energy to be transmitted through the specimen.

C) Effect of the pressure on the couplant efficiency - An improved signal can be obtain by applying a certain amount of hand pressure on the transducers.

In the experiment, three cores of 1½" dia by 4" length were drilled from the three direction of the blocks. Ends were machined flats and made parallel. Two types of couplant oils were used. For compressional wave velocity, the ordinary vaselline was quite sufficient for transmitting the P-wave, but this oil was not sufficient for shear S-wave, since S-wave is retarded considerably through air. A better cementing couplant, of the sample to the transducers was made by using the extremely SBEL viscons grease. It is high competent and does not decrease the energy of shear waves. The results of the test are given in the table.

Conclusions

The presented table of the physical properties of rock from Iraq is the first of its kind and can be part of a series to cover all rock types and rock formations in the country. Certain facts have emerged from the experimental part of this article. These are outlined here:-

I) For determination of the saturated densities, it is suggested that samples should be saturated under vacum to insure full saturation.

II. For determing the high and low magnetic susceptibility rocks, both in the laboratory as well as in the field, the Kappa-meter found to be a valuable tool, due to its sensitivity, and applicability.

III. Observation of the electrical resistivity results, above that there were variation among (A) samples of different rock types, and (B) samples of the same rock (quasi-homogeneous) types. For the last, the range of reading was taken for a particular type of rock (ex-gypsum). For dense hard rocks, the results of tests on three samples were almost identical and hence average was taken, (ex-galala marble).

IV. The securacy of measurements of P- and S-wave velocities depends primarily on the quality of the received signal, the best possible signal should be obtained for each sample. This involves insuring that proper alignment of transducers, coupling, samples surface smoothness and parallelism is obtained. In some cases it may be necessary to reduce the length to achieve a good quality signal, whenever possible sample diameter should not be less than transducer diameter.

In samples of Loose material (e.g. coarse grained friable Gercus sandstone, the absorption of the elastic energy is appreciable and the impulse arriving at the sensing device (Oscilloscope) was too weak to be detected & hence no results of P & S wave velocities were obtained.

V. It was found quite difficult to drill cores from the incompetent friable rock like Gaars Sandstone and Upper Fars Sandstone,

this was either due to their great Friability, also due using water as coolant drilling agent. It may be possible to drill core from them by using pumped air system instead of water, that was not available with the heavy duty coring machine available in our laboratory. Therefore no result of P, S, results was made for them.

Acknowledgement

This work was conducted in the laboratory of rock machines and Engineering geology of the department of applied geology, Al-Mustansiriyah University.

References

1) S.S. West, 1941 - The density on seismic reflections Journal of Geophsics, Vol. VI, No. 1, p45-51.

2) J.R., Balslely, and A.F. Buddington, Magnetic susceptibility and fabric of some Adirondack granites and orthogneiss, American Journal of Science, v. 258, No. 6. (1960).

3) H.M. Mooney, and Bleifuss, Magnetic Susceptibility measurements in Minnesota, Journal of Geophysics, U.K., p. 383. (1953).

4) C.V. Killer, and Frischknecht,"Electrical methods in geophysical prospecting" Pergamon Press. (1970).
"Electrical methods in geophysical Prospecting" Pergamon Press.

5) E.I. Parkhomenko, Electrical properties of rocks publisher plenum press, N.Y. (1967).

6) L.Y. Faust, Seismic velocity as a function of depth and geologic time, Journal of Geophysics, Vol. 16, p 192-206. (1951).

THE LEAST SQUARE ESTIMATES AND THE PROBLEM OF MISSING VALUES IN THE LINEAR MODELS

A. S. El-Aloosy and A.M. Haider*

A B S T R A C T

Where as the statistical theory of parameter estimation in linear models is almost completely developed, the problem of using incomplete data for such estimates has not yet been solved successfully. However, some statistican suggested the use of prediction of the missing data to complete the incomplete available data. This completed data in another round to be used in estimating the parameters required. In this paper we proved that, in linear models using the Least Square method, and the completed data does not give better estimates. In fact using completed data or incomplete data lead to the same estimates.

Mathematical Development of the Theory:-

Let $\vec{Y} = \underset{\wedge}{X}\vec{\theta} + \vec{\epsilon}$ (2.1)

to represent the general linear model we use, where: $\vec{Y}$, is a random vector of order x x 1, and $\underset{\wedge}{X}$ is a constant matrix of order n x p, and $\vec{\theta}$ is a vector of parameters to be estimated of order p x 1. also, we have:

$E\vec{Y} = \underset{\wedge}{X}\vec{\theta}$, where

$E\vec{\epsilon} = \vec{\emptyset}$ a null vector of order n x 1 , and

*. Department of statistics, Al-Mustansiriyah University, Baghdad - IRAQ.

$\text{Cov } \vec{Y} = \text{Cov } \vec{\epsilon} = \underset{\wedge}{\Sigma}$, is a positive definite matrix of rank n. We assume:

$\vec{Y} = \begin{pmatrix} \vec{Y}_1 \\ \vec{Y}_2 \end{pmatrix}$, where $\vec{Y}_1$, $\vec{Y}_2$ are subvectors of $\vec{Y}$, of orders k x 1 and n-k x 1 respectively and:

$\text{Cov } \vec{Y}_1 = \underset{\wedge}{\Sigma}_{11}$ is a positive definite matrix of rank k, and

$\text{Cov } \vec{Y}_2 = \underset{\wedge}{\Sigma}_{22}$ is a positive definite matrix of rank n - k, and we assume:

$$\underset{\wedge}{\Sigma} = \begin{pmatrix} \underset{\wedge}{\Sigma}_{11} & \underset{\wedge}{\emptyset}_{12} \\ \underset{\wedge}{\emptyset}_{21} & \underset{\wedge}{\Sigma}_{22} \end{pmatrix}$$, where $\underset{\wedge}{\emptyset}_{12}$, $\underset{\wedge}{\emptyset}_{21}$ are null matrices of orders k x (n-k) and (n-k)x k respectively. Also, we define $\underset{\wedge}{X}_1$, $\underset{\wedge}{X}_2$ as two constant matrices of order k x p and (n - k) x p respectively, and

$\underset{\wedge}{X}' = (\underset{\wedge}{X}_1' \ \underset{\wedge}{X}_2')$, where $\underset{\wedge}{X}'$ means transpose of $\underset{\wedge}{X}$.

Thus (2,1) may be written as:

$$\begin{pmatrix} \vec{Y}_1 \\ \vec{Y}_2 \end{pmatrix} = \begin{pmatrix} \underset{\wedge}{X}_1 \\ \underset{\wedge}{X}_2 \end{pmatrix} \vec{\theta} + \begin{pmatrix} \vec{\epsilon}_1 \\ \vec{\epsilon}_2 \end{pmatrix} \qquad (2.2)$$

If we assume $\vec{Y}_1$ to be the missed data, then we can write:

$$\vec{Y}_2 = \underset{\wedge}{X}_2 \vec{\theta} + \vec{\epsilon}_2 \qquad (2.3)$$

using generalized least square method, we obtain

$$\hat{\vec{\theta}} = (\underset{\wedge}{X}_2' \underset{\wedge}{\Sigma}^{-1}_{22} \underset{\wedge}{X}_2)^{-1} \; \underset{\wedge}{X}_2' \underset{\wedge}{\Sigma}^{-1}_{22} \vec{Y}_2 \qquad (2.4)$$

We may write:

$$\underset{\wedge}{X}_2' \underset{\wedge}{\Sigma}^{-1}_{22} \underset{\wedge}{X}_2 = \underset{\wedge}{X}' \underset{\wedge}{\Sigma}^{-1} \underset{\wedge}{X} - \underset{\wedge}{X}_1' \underset{\wedge}{\Sigma}^{-1}_{11} \underset{\wedge}{X}_1 \qquad (2.5)$$

Using (2.4) , (2.5) and applying lemma 1 in the appendix; It is easily seen that (2.4) can be written as follows:(*)

$$\hat{\vec{\theta}} = \left[(\underset{\wedge}{X}' \underset{\wedge}{\Sigma}^{-1} \underset{\wedge}{X})^{-1} - (\underset{\wedge}{X}' \underset{\wedge}{\Sigma}^{-1} \underset{\wedge}{X})(-\underset{\wedge}{X}_1) \underset{\wedge}{C} \underset{\wedge}{\Sigma}^{-1}_{11} \underset{\wedge}{X}_1 (\underset{\wedge}{X}' \underset{\wedge}{\Sigma}^{-1} \underset{\wedge}{X})^{-1} \right] \times$$

$$(\underset{\wedge}{X}_2' \underset{\wedge}{\Sigma}^{-1}_{22} \vec{Y}_2) , \qquad (2.6)$$

Where:

$$\underset{\wedge}{C} = (\underset{\wedge}{I} - \underset{\wedge}{\Sigma}^{-1}_{11} \underset{\wedge}{X}_1 \; (\underset{\wedge}{X}' \underset{\wedge}{\Sigma}^{-1} \underset{\wedge}{X})^{-1} \; \underset{\wedge}{X}_1')^{-1}$$

$$\hat{\vec{\theta}} = (\underset{\wedge}{X}' \underset{\wedge}{\Sigma}^{-1} \underset{\wedge}{X})^{-1} \left[\underset{\wedge}{I} + \underset{\wedge}{X}_1' \; \underset{\wedge}{C} \underset{\wedge}{\Sigma}^{-1}_{11} \underset{\wedge}{X}_1 \; (\underset{\wedge}{X}' \underset{\wedge}{\Sigma}^{-1} \underset{\wedge}{X})^{-1} \right] \text{ times}$$

$$(\underset{\wedge}{X}_2' \underset{\wedge}{\Sigma}^{-1}_{22} \vec{Y}_2); \qquad (2.7)$$

Therefore: the predicted missing values $\hat{\vec{Y}}_1^*$ can be expressed as:

$$\hat{\vec{Y}}_1^* = \underset{\wedge}{X}_1 \hat{\vec{\theta}} \qquad (2.8)$$

$$= \underset{\wedge}{X}_1 (\underset{\wedge}{X}' \underset{\wedge}{\Sigma}^{-1} \underset{\wedge}{X})^{-1} \left[\underset{\wedge}{I} + \underset{\wedge}{X}_1 \underset{\wedge}{C} \underset{\wedge}{\Sigma}^{-1}_{11} \underset{\wedge}{X}_1 (\underset{\wedge}{X}' \underset{\wedge}{\Sigma}^{-1} \underset{\wedge}{X})^{-1} \right] \text{ times}$$

$$(\underset{\wedge}{X}_2' \underset{\wedge}{\Sigma}^{-1}_{22} \vec{Y}_2)$$

* See the appendix.

$$= \left[\underset{\sim}{\Sigma}_{11}^{-1} \underset{\sim}{C}^{-1} + \underset{\sim}{X}_1 \left(\underset{\sim}{X}' \underset{\sim}{\Sigma}^{-1} \underset{\sim}{X} \right)^{-1} \underset{\sim}{X}_1' \right] \underset{\sim}{C} \underset{\sim}{\Sigma}_{11}^{-1} \underset{\sim}{X}_1 \quad \text{times}$$

$$\left(\underset{\sim}{X}' \underset{\sim}{\Sigma}^{-1} \underset{\sim}{X} \right)^{-1} \underset{\sim}{X}_2' \underset{\sim}{\Sigma}_{22}^{-1} \vec{Y}_2 \qquad (2.9)$$

Hence, by using (2.6), (2.9) we obtain:

$$\hat{\vec{Y}}_1^* = \left\{ \underset{\sim}{\Sigma}_{11} \left[\underset{\sim}{I} - \underset{\sim}{\Sigma}_{11}^{-1} \underset{\sim}{X}_1 \left(\underset{\sim}{X}' \underset{\sim}{\Sigma}^{-1} \underset{\sim}{X} \right)^{-1} \underset{\sim}{X}_1' \right] + \underset{\sim}{X}_1 \left(\underset{\sim}{X}' \underset{\sim}{\Sigma}^{-1} \underset{\sim}{X} \right)^{-1} \right\} \text{times}$$

$$\left\{ \underset{\sim}{C} \underset{\sim}{\Sigma}_{11}^{-1} \underset{\sim}{X}_1 \left(\underset{\sim}{X}' \underset{\sim}{\Sigma}^{-1} \underset{\sim}{X} \right)^{-1} \underset{\sim}{X}_2' \underset{\sim}{\Sigma}_{22}^{-1} \vec{Y}_2 \right\} \qquad (2.10)$$

However, if we write:

$\vec{Y}^* = \begin{pmatrix} \hat{\vec{Y}}_1^* \\ \vec{Y}_2 \end{pmatrix}$, then: the estimates $\hat{\vec{\theta}}^*$ using $\hat{\vec{Y}}^*$ are:

$$\hat{\vec{\theta}}^* = \left(\underset{\sim}{X}' \underset{\sim}{\Sigma}^{-1} \underset{\sim}{X} \right)^{-1} \underset{\sim}{X}' \underset{\sim}{\Sigma}^{-1} \vec{Y}^*$$

$$= \left(\underset{\sim}{X}' \underset{\sim}{\Sigma}^{-1} \underset{\sim}{X} \right)^{-1} \left(\underset{\sim}{X}_1' \underset{\sim}{X}_2' \right) \begin{pmatrix} \underset{\sim}{\Sigma}_{11}^{-1} & \underset{\sim}{\phi}_{12} \\ \underset{\sim}{\phi}_{21} & \underset{\sim}{\Sigma}_{22}^{-1} \end{pmatrix} \begin{pmatrix} \hat{\vec{Y}}_1^* \\ \vec{Y}_2 \end{pmatrix}$$

$$= \left(\underset{\sim}{X}' \underset{\sim}{\Sigma}^{-1} \underset{\sim}{X} \right)^{-1} \left(\underset{\sim}{X}_1 \underset{\sim}{\Sigma}_{11}^{-1} \vec{Y}_1^* + \underset{\sim}{X}_2 \underset{\sim}{\Sigma}_{22}^{-1} \vec{Y}_2 \right) \qquad (2.11)$$

Hence:

$$\hat{\vec{\theta}}^* \left(\underset{\sim}{X}' \underset{\sim}{\Sigma}^{-1} \underset{\sim}{X} \right)^{-1} \left[\left(\underset{\sim}{X}_1' \underset{\sim}{\Sigma}_{11}^{-1} \underset{\sim}{\Sigma}_{11} \underset{\sim}{C} \underset{\sim}{\Sigma}_{11}^{-1} \underset{\sim}{X}_1 \right) \text{times} \right.$$

$$\left. \left(\underset{\sim}{X}' \underset{\sim}{\Sigma}^{-1} \underset{\sim}{X} \right)^{-1} \underset{\sim}{X}_2' \underset{\sim}{\Sigma}_{22} \vec{Y}_2 \right) + \underset{\sim}{X}_2' \underset{\sim}{\Sigma}_{22}^{-1} \vec{Y}_2 \Big]$$

$$= \left(\underset{\sim}{X}' \underset{\sim}{\Sigma}^{-1} \underset{\sim}{X} \right)^{-1} \left[\underset{\sim}{X}_1' \underset{\sim}{C} \underset{\sim}{\Sigma}_{11}^{-1} \underset{\sim}{X}_1 \left(\underset{\sim}{X}' \underset{\sim}{\Sigma}^{-1} \underset{\sim}{X}^{-1} \right) \text{times} \right.$$

$$\left. \underset{\sim}{X}_2' \underset{\sim}{\Sigma}_{22}^{-1} \vec{Y}_2 + \underset{\sim}{X}_2 \underset{\sim}{\Sigma}_{22}^{-1} \vec{Y}_2 \right] ,$$

$$= (\underset{\wedge}{X}' \underset{\wedge}{\Sigma}^{-1} \underset{\wedge}{X})^{-1} \left[\underset{\wedge}{X}_1' \; C \underset{\wedge}{\Sigma}_{11}^{-1} \underset{\wedge}{X}_1 \quad \text{times} \right.$$

$$\left. (\underset{\wedge}{X}' \underset{\wedge}{\Sigma}^{-1} \underset{\wedge}{X})^{-1} \underset{\wedge}{X}_2' \underset{\wedge}{\Sigma}_{22}^{-1} \vec{Y}_2 + \underset{\wedge}{X}_2 \underset{\wedge}{\Sigma}_{22}^{-1} \vec{Y}_2 \right] ,$$

$$= (\underset{\wedge}{X} \underset{\wedge}{\Sigma}^{-1} \underset{\wedge}{X})^{-1} \left[\underset{\wedge}{X}_1' C \underset{\wedge}{\Sigma}_{11}^{-1} \underset{\wedge}{X}_1 (\underset{\wedge}{X}' \underset{\wedge}{\Sigma}^{-1} \underset{\wedge}{X})^{-1} + I \right] \text{ times}$$

$$(\underset{\wedge}{X}_2' \underset{\wedge}{\Sigma}_{22}^{-1} \vec{Y}_2) \qquad (2.12)$$

Therefor: from (2.7) and (2.12) above we conclude that

$$\hat{\vec{\theta}}^* = \vec{\theta} \qquad (2.13)$$

Furthermore; If R.S.S. $\hat{\vec{\theta}}^*$ = Residual sum of squares using completed data, and if R.S.S $\hat{\vec{\theta}}$ = Residual sum of square using the incomplete data only; then:

$$\text{R.S.S } \hat{\vec{\theta}}^* = \vec{Y}^{*\prime} \vec{Y}^* - \vec{Y}^{*\prime} \underset{\wedge}{X} \hat{\vec{\theta}}^* \qquad (2.14)$$

and

$$\text{R.S.S } \hat{\vec{\theta}} = \vec{Y}_2' \vec{Y}_2 - \vec{Y}_2' \underset{\wedge}{X}_2 \hat{\vec{\theta}} \qquad (2.15)$$

But since:

$$\text{R.S.S } \hat{\vec{\theta}}^* = \vec{Y}^{*\prime} \vec{Y}^* - \vec{Y}^{*\prime} \underset{\wedge}{X} \hat{\vec{\theta}}^*$$

$$= \hat{\vec{Y}}_1^{*\prime} \hat{\vec{Y}}_1^* + \vec{Y}_2' \vec{Y}_2 - \hat{\vec{Y}}_1' \underset{\wedge}{X}_1' \hat{\vec{\theta}}^* - \vec{Y}_2' \underset{\wedge}{X}_2 \hat{\vec{\theta}}^* \; ;$$

Hence:

$$\text{R.S.S } \hat{\vec{\theta}}^* = \vec{Y}_2' \vec{Y}_2 - \vec{Y}_2' \underset{\wedge}{X}_2 \hat{\vec{\theta}}^* + \hat{\vec{Y}}_1' (\hat{\vec{Y}}_1 - \underset{\wedge}{X}_1 \hat{\vec{\theta}}^*)$$

By using (2.13) we can obtain:

$$\text{R.S.S } \hat{\vec{\theta}}^* = \vec{Y}_2' \vec{Y}_2 - \vec{Y}_2' \underset{\wedge}{X}_2 \hat{\vec{\theta}}^* + \hat{\vec{Y}}_1' (\vec{Y}_1 - \underset{\wedge}{X}_1 \hat{\vec{\theta}}^*) ,$$

and by using (2.8), $\text{R.S.S } \hat{\vec{\theta}} = \vec{Y}_2' \vec{Y}_2 - \vec{Y}_2' \underset{\wedge}{X}_2 \hat{\vec{\theta}}$

Hence, from (2.15) and (2.16) we conclude that:

Hence: $$\text{R.S.S } \hat{\vec{\theta}}^* = \text{R.S.S } \hat{\vec{\theta}}^* \qquad (2.17)$$

3. Conclusion:-

It has been proved that no improvement in estimates is detected as a consequence of using to completed data over estimates obtained from the incomplete data available. These results are true only when using Lease Square estimates in the linear models, when incompleteness is due to a design rather due to random effects.

However, further problems are left for further investigations. The problems are: Estimating parameters in the linear models when other estimation procedures are to be used beside the Least Square method, considering missing data due to random effects rather then due to a design.

APPENDIX

LEMMA (1).

If $\underset{\wedge}{\Sigma} = \underset{\wedge}{A} + \underset{\wedge}{B}\underset{\wedge}{D}$, then :

$$\underset{\wedge}{\Sigma}^{-1} = \underset{\wedge}{A}^{-1} + \underset{\wedge}{A}^{-1}\ \underset{\wedge}{B}\ \underset{\wedge}{C}\ \underset{\wedge}{D}\ \underset{\wedge}{A}^{-1} ,$$

Where $\underset{\wedge}{C} = -\left(\underset{\wedge}{I} + \underset{\wedge}{D}\ \underset{\wedge}{A}^{-1}\ \underset{\wedge}{B}\right)^{-1}$

Application of Lemma (1):-

From equations (2.4) and (2.5) we obtain

$$\underset{\wedge}{\vec{\theta}} = \left[\underset{\wedge}{X}' \underset{\wedge}{\Sigma}^{-1} \underset{\wedge}{X} - \underset{\wedge}{X}_1 \underset{\wedge}{\Sigma}_{11}^{-1} \underset{\wedge}{X}_1\right]^{-1} \underset{\wedge}{X}_2' \underset{\wedge}{\Sigma}_{22}^{-1} \underset{\wedge}{\vec{Y}}_2$$

If we use in Lemma (1) ,

$$\underset{\wedge}{A} = \underset{\wedge}{X}' \underset{\wedge}{\Sigma}^{-1} \underset{\wedge}{X} ,$$

$$\underset{\wedge}{B} = -\underset{\wedge}{X}_1'$$

and

$$\underset{\wedge}{D} = \underset{\wedge}{\Sigma}_{11}^{-1} \underset{\wedge}{X}_1$$

then (2.6) is easily obtained:

REFERENCES

1. A.A. Afifi and R.M. Elashoff, "Missing observations in Multivariate statistics", I Review of Literature, Journal of American Statistical Assoc. pp(595). (1966).

2. F.S. Buck, "A Method of estimation of missing values in multivariate data suitable for use with an Electronic Computer", Journal of Royal Statistical Society, Serier B, 22, pp(302). (1969).

3. A. Matthal, "Estimation of parameters from incomplete data with application to design of sampling survey", Senkhya 11, pp(145. (1951).

4. S.J. Press, Applied multivariate analysis, Publisher Holt, Rinehart and Winston Inc., pp(23) (1972).

5. K.D. Tocher, "The design and analysis of block experiment", Journal Royal Statistical Society, Series B, 14, pp(45-100) (1952).

6. M. Woodbury, Technical report No. 42; Princeton University, Princeton, N.J., U.S.A.

DECAY SCHEME STUDIES IN ^{152}Sm

B.A. Bishara*, M.A. Al-Jeboori*, and K.F. Kaddoumi*

A B S T R A C T

The gamma-rays emitted in the decay of $^{152}Eu^{g}$ have been studied by high efficiency, high-resolution, solid-state detectors. These measurements together with Ge(Li)- Ge(Li) coincidence experiments revealed the existence of 58 gamma transitions in the decay of ^{152}Sm. The coincidence work confirmed the existence of the new levels at 1680.0 and 1701.4 keV in ^{152}Sm. The measurement of the annihilation radiation showed that the positron branch intensity is (0.016 ± 0.003)% of the total decay. The nature of the excited states are discussed qualitatively and are assorted into the different rotation-vibration bands.

I N T R O D U C T I O N

The onset of nuclear deformation is rather abrupt at the beginning of the rare-earth region of deformed nuclei. The N=90 nuclei, e.g. ^{152}Sm, display the low-lying excited states characteristic of rotational spectra and are considered to be deformed. However, this nucleus is better referred to as transitional, since its properties preclude classification as a deformed nucleus.

---

* Department of Physics, College of Science, Al-Mustansiriyah University, Baghdad, IRAQ.

Al-Mustansiriyah Journal of Science, Vol.4, No.2 (1979).

The nuclear decay scheme of ^{152}Sm has been the subject of several investigations from the decay of the $^{152}Eu^{m,g}$ isomeric pair [1] , charged particle experiments [2,3] , and Coulomb excitation experiments [4] . Several investigations of the decay of ^{152}Eu [5 - 7] have revealed several high energy levels and several weak gamma transitions in the decay of ^{152}Sm, but the reported results show some differences. At this stage, it is felt that a thorough revision is needed for a detailed investigation of the decay of $^{152}Eu^{g}$. This has been accomplished by using a high energy-resolution and high efficiency Ge(Li) spectrometer and extensively employing Ge(Li) - Ge(Li) coincidence techniques in order to make sure of the excited states of ^{152}Sm and establish the correct placements of transitions between the different bands.

EXPERIMENTAL PROCEDURE

The $^{152}Eu^{g}$ source is obtained from a commercial supplier (Radiochemical Centre Amersham, England.) in the form of a point source with activity of about ten microcuries. The only impurity found is approximately 1% of ^{154}Eu which presented little difficulty in the analysis of the spectra since its decay features are well known [12] .

Two lithium-drifted germanium detectors (Ortec model 81) are used in singles and coincidence measurements. Each detector is true coaxial right-angle system with activ. volume of 102.8 cm^3. The optimum energy resolution of the detector is 2.1 keV FWHM at 1332 keV and a peak-to-Compton ratio of 41 to 1.

A variety of electronics is used to obtain the data where all of it consists of Ortec preamplifiers, amplifiers, single channels, linear gates, coincidence units, and time-to-pulse-height converter (see Fig. 1). All spectra are recorded on a 1024 channel multi-channel analyzer, (Ortec model 6240 B) with digitizing rate of 100 MHZ, which is connected to a teletype and an X-Y plotter. The data of the singles and coincidences spectra are analyzed by hand. Larger errors are given to the energies and intensity measurements than would have been if an extensive computer alysis had been performed.

R E S U L T S

A. Gamma Singles Spectrum

The gamma-ray singles spectrum of the decay of $^{152}Eu^{g}$ is measured by the single channel of the system shown in Fig.1, where the source is located at a distance of about 15 cm from the face of the detector to reduce the summing effects. To study the details of the singles spectrum, it has been divided into four parts, Figs. 2 to 5 show a typical gamma spectrum of ^{152}Eu which includes all the transitions in the decays of both ^{152}Sm and ^{152}Gd.

The energies are determined by using a calibration set of standard reference sources, and the well-known intense gamma lines of ^{152}Eu are also used as internal standards. The errors in the energy determination are estimated to range between 0.09% to 0.66% for the energies below 1 MeV, and between 0.05% to 0.08% for the energy range 1.0 to 1.7 MeV. Table 1 gives the

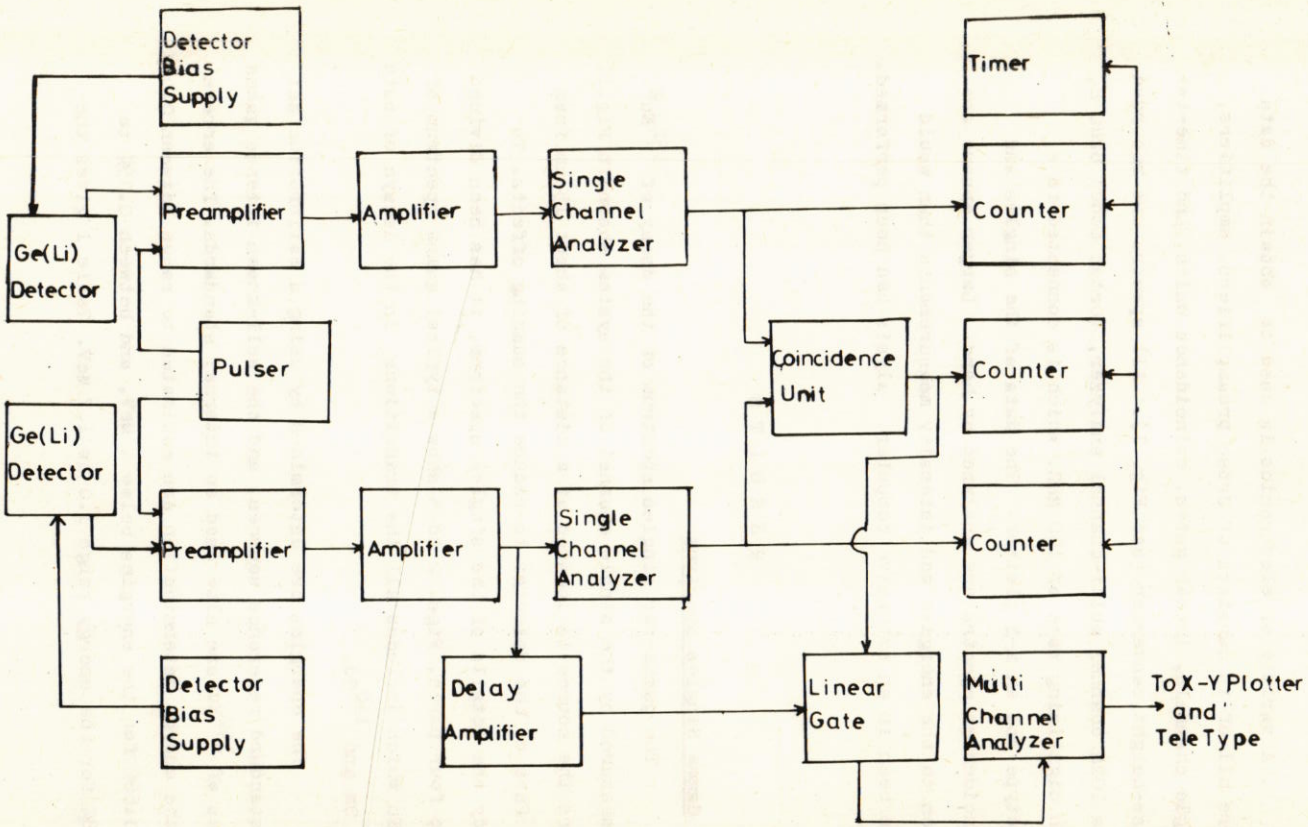

FIG.(1) GAMMA-GAMMA COINCIDENCE SYSTEM USING TWO Ge(Li) DETECTORS

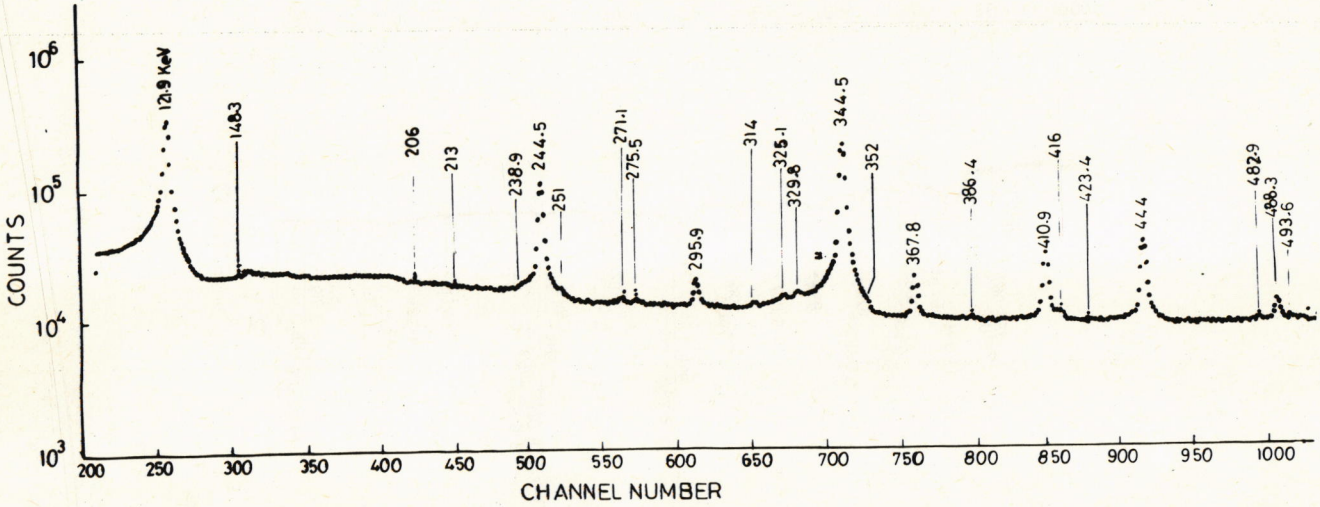

FIG.(2) LOW ENERGY PORTION OF THE Eu^{152} GAMMA RAY SPECTRUM TAKEN WITH Ge(Li) DETECTOR.

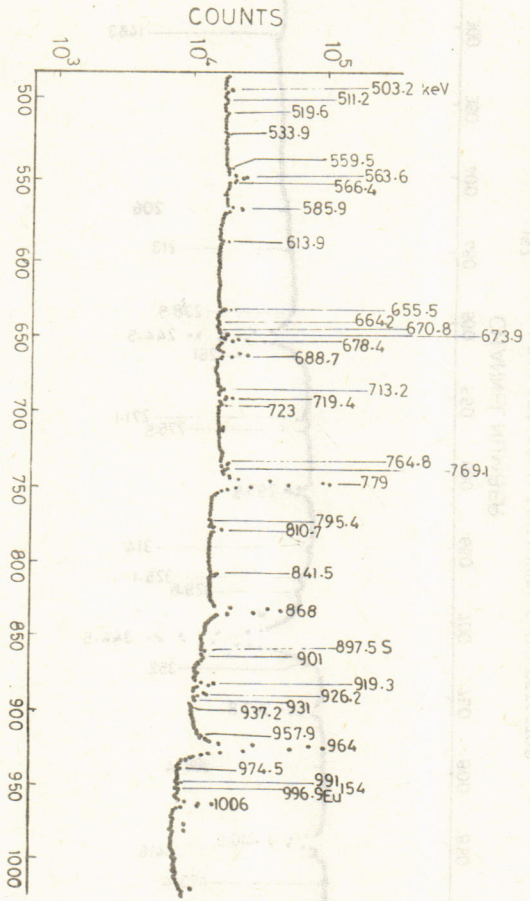

FIG.(3) LOW ENERGY PORTION OF THE Eu^{152} GAMMA RAY SPECTRUM TAKEN WITH Ge(Li) DETECTOR

THE ENERGY SUFFIXED BY S DENOTES SINGL ESCAPE PEAK.

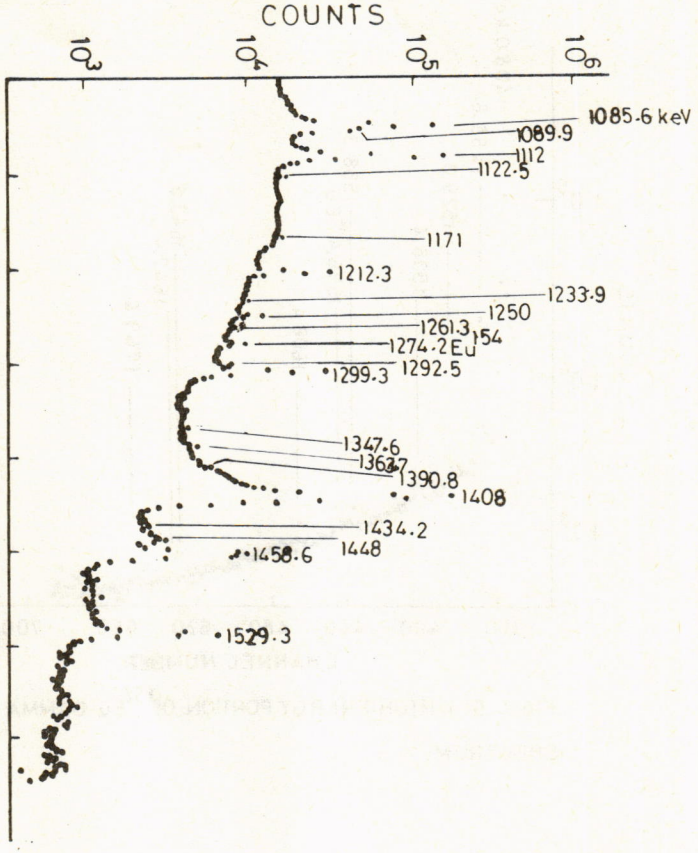

FIG. (4.) HIGH ENERGY PORTION OF THE EU^{152} GAMMA RAY SPECTRUM TAKEN WITH Ge(Li) DETECTOR

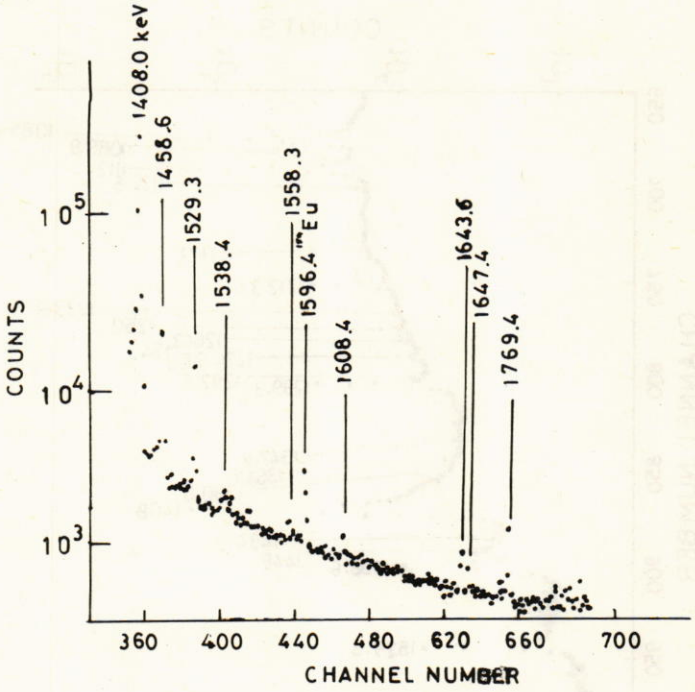

FIG.(5) HIGH-ENERGY PORTION OF ^{152}Eu GAMMA RAY SPECTRUM.

gamma lines of the decay of ^{152}Sm as compared with data of other authors [5 -7] .

Table 1. Energies of gamma rays (in keV) emitted in the decay of ^{152}Sm

Present Study	Riedinger (ref.5)	Varnell (ref.6)	Baker (ref.7)
121.9	121.77	121.8	121.78
148.3			148.0
206.0			207.4
213.0	212.4		212.4
238.9			238.8
244.5	244.69	244.7	244.6
251.0	251.7		251.62
			269.4
275.5	275.6	275.4	275.4
285.9			285.8
295.9	296.0	295.9	295.9
			316.0
329.8	329.4		329.41
			330.9
			340.5
386.4			385.7
416.0	416.2		416.07
423.4			423.7
444.0	444.0	444.1	444.0
482.9	482.8		482.7

Present Study	Riedinger (ref.5)	Varnell (ref.6)	Baker (ref.7)
486.3	488.7	488.4	488.46
493.6	493.7	493.6	493.6
496.0*			496.3
			523.2
			535.3
559.5			556.5
			561.0
563.6	564.0	563.8	563.97
566.4	566.8	566.3	566.5
613.9			616.9
			644.3
655.5	656.5	656.5	656.51
664.2			664.3
670.8	671.3		671.3
673.9	674.7	674.7	674.6
			686.8
688.7	688.6	688.7	688.6
719.4	719.3	719.4	719.4
723.0			727.9
769.1	769.3	769.2	769.15
			805.7
810.7	810.4	810.7	810.51
			839.7
841.5	841.4	841.8	841.4
868.0	867.32	867.7	867.39
901.0	901.2	901.0	901.04

Present Study	Riedinger (ref.5)	Varnell (ref.6)	Baker (ref.7)
919.3	919.3	919.7	919.4
			919.6
926.2	926.2		926.22
957.9			959.5
963.4			963.4
964.0	964.03	964.7	964.0
1006.0	1005.0	1005.0	1005.06
1085.6	1085.79	1086.0	1085.8
1112.0	1112.05	1112.2	1112.07
1171.0	1171.0		1171.0
1212.3	1212.8	1212.8	1212.89
1250.0	1249.8	1249.7	1249.8
1292.5	1292.6		1292.74
1316.5			1313.5
1335.0			1334.3
1363.7	1363.7		1363.84
1390.8			1390.4
1408.0	1408.04	1408.1	1408.08
1458.6	1457.6	1458.3	1457.95
1529.3	1528.0	1529.8	1528.65
1558.3			1558.2
1608.4	1608.2		1608.33
1647.4	1647.5		1647.33
1769.4	1769.3		1769.13

* Energy determined from coincidence measurements.

B. Intensity Determination

Relative gamma-ray intensities are determined by summing the counts under each photopeak after subtracting the background. The final results are corrected for the efficiency of the detector. The results are summarized in Table 2 where the relative intensities of the gamma lines in ^{152}Sm are given relative to the intense 344.5 keV line of ^{152}Gd which is considered to have an intensity of 100. The intensity of the 1006.0 keV line has been reduced by 25% to correct for the contribution of the intense 1004.75 keV line of ^{154}Eu.

C. Coincidence Spectra

In order to separate the gamma-ray transitions belonging to ^{152}Sm from those of ^{152}Gd, and to place the gamma transitions into their proper locations in ^{152}Sm level scheme, the coincidence measurements are carried out using the coincidence spectrometer shown in Fig.1. Seven gates set on transitions in ^{152}Sm are used to verify the placements of the gamma transitions in the decay scheme (Fig.6). Table 3 gives a listing of the coincidence relationships obtained from these gates. Careful checks are taken against electronic drifts, chance coincidence, and also the unreal coincidence due to the Compton background under the peak of the gate. The doublet nature of some of the lines (e.g. 444.0 - 444.0 and 963.4-964 keV) requires special care in analyzing their coincidences.

Several coincidence spectra at different gates are shown in the Figs. 7 to 11 to illustrate some of the results

obtained from coincidence work. Fig. 7 displays the 121.9 keV gated spectrum where nearly all the gamma transitions in coincidence with 121.9 keV transition are observed. Only two transitions, namely the 719.4 and 769.1 keV lines, are not clear in the figure, while they are seen in coincidence with 244.5 and 444.0 keV lines. In Fig. 10, which shows the coincidence spectrum with the 1085.6 keV gate, the presence of the 344.5 keV line which belongs to ^{152}Gd is due to the presence of the 1089.9 keV line in the gate. It is worth noting that the 496.0 keV gamma-ray, which has not been seen in the singles spectrum, is detected in the coincidence spectrum gated by the 1112.0 keV line (see Fig. 11).

The results of the singles and coincidence measurements are shown in the decay scheme of ^{152}Sm (Fig. 6). All the energy states are confirmed in the present work, but some few transitions are still doubtful, and are indicated by dashed lines in the figure, since they could not be observed in the present study.

Table 2. Energies and relative intensities of gamma rays emitted in the decay of ^{152}Sm

Energy (keV)	Relative Intensity
121.9	108.6 ± 3.000
148.3	≤ 0.010
206.0	0.024 ± 0.01
213.0	0.08 ± 0.013

Energy (keV)	Relative Intensity
238.9	0.31 ± 0.09
244.5	29.22 ± 0.61
251.0	0.301± 0.024
275.5	0.21 ± 0.01
285.9	0.021± 0.003
295.9	1.61 ± 0.1
329.8	0.395± 0.26
386.4	0.076± 0.016
416.0	0.36 ± 0.043
423.4	≤ 0.2
444.0	10.43 ± 0.46
482.9	0.14 ± 0.04
488.3	1.5 ± 0.1
493.6	0.16 ± 0.032
496.0	≤ 0.05
559.5	0.053± 0.02
563.6	1.82 ± 0.09
566.4	0.402± 0.02
613.9	0.043± 0.01
655.5	0.60 ± 0.02
664.2	0.021± 0.001
670.8	0.05 ± 0.01
673.9	0.50 ± 0.02
688.7	3.1 ± 0.1
719.4	1.14 ± 0.11
723.0	0.0318± 0.009

Energy (keV)	Relative Intensity
769.1	0.32 ± 0.30
810.7	1.12 ± 0.31
841.5	0.70 ± 0.04
868.0	16.01 ± 0.10
901.0	0.29 ± 0.09
919.3	1.51 ± 0.12
926.2	0.867± 0.10
957.9	0.041± 0.02
963.4	0.36 ± 0.05
964.0	50.8 ± 1.3
1006	2.325± 0.14
1085.6	35.70 ± 0.13
1112.0	49.51 ± 0.80
1171	0.141± 0.021
1212.3	4.64 ± 0.20
1250.0	0.67 ± 0.05
1292.5	0.41 ± 0.03
1316.5	0.02 ± 0.003
1335.0	0.018± 0.003
1363.7	0.11 ± 0.011
1390.8	0.021± 0.003
1408.0	80.40 ± 0.15
1458.6	1.91 ± 0.13
1529.3	1.211± 0.10
1558.3	0.0029±0.002
1608.4	0.025± 0.001
1647.41	0.02 ± 0.005
1769.4	0.035± 0.002

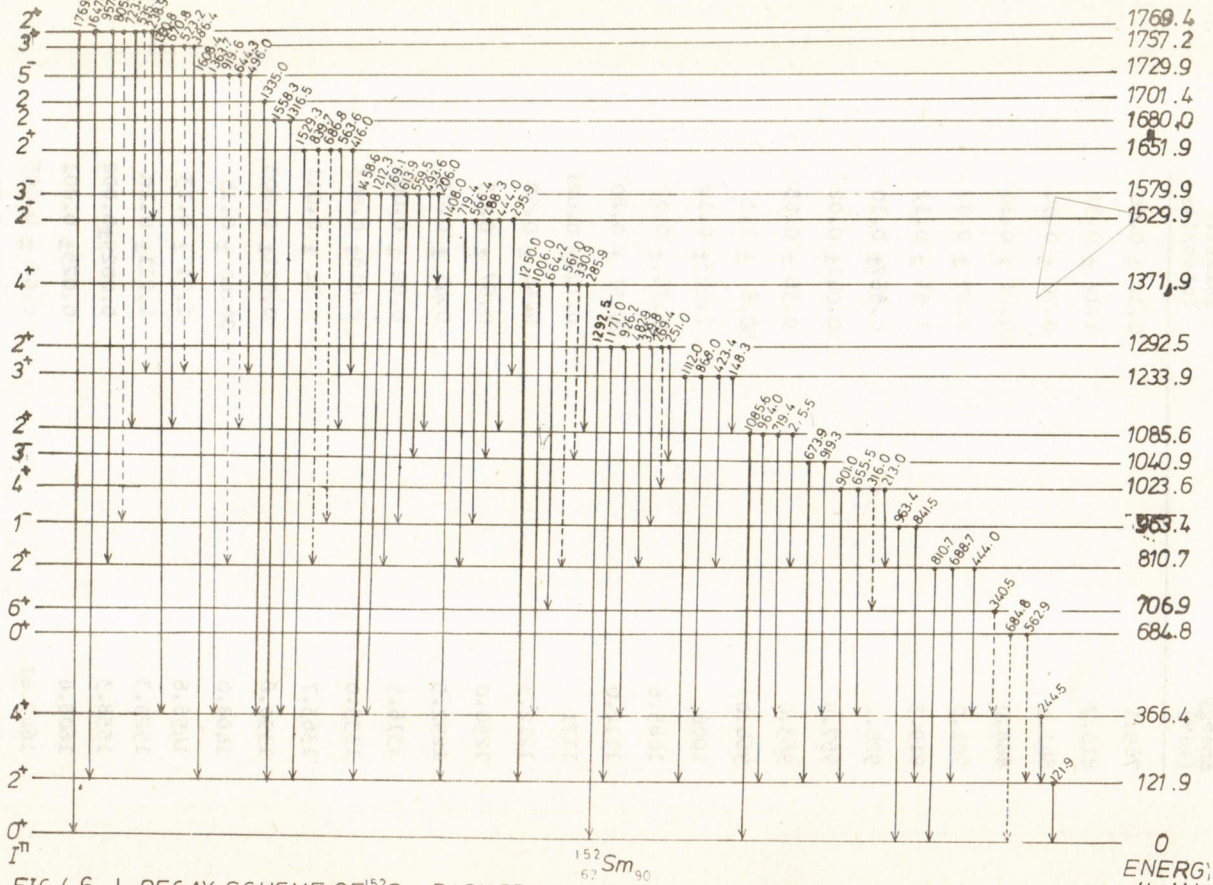

FIG.(6) DECAY SCHEME OF ^{152}Sm. DASHED LINES INDICATES UNOBSERVED TRANSITIONS

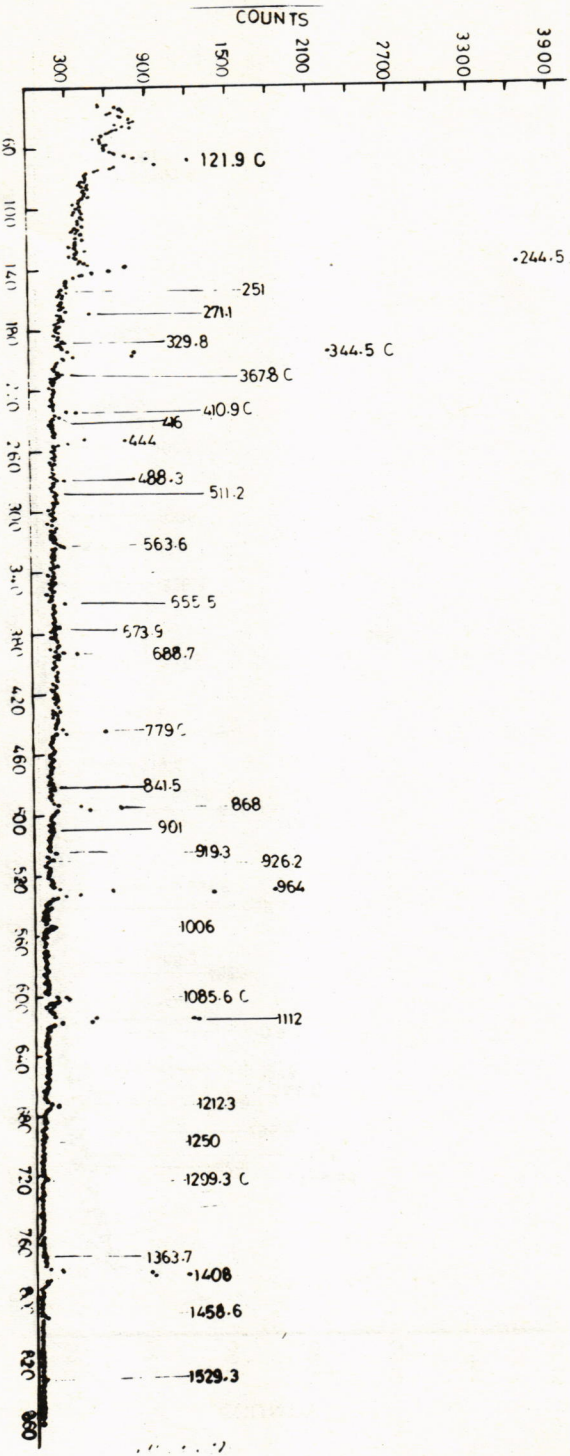

FIG. (7) GAMMA RAY SPECTRUM OF Eu^{152} IN COINCIDENCE WITH 121.9 KeV TRANSITION

ENERGIES SUFFIXED BY C ARISE FROM CHANCE COINCIDENCE

FIG.(8) GAMMA RAY SPECTRUM OF Eu^{152} IN COINCIDENCE WITH 244.5keV TRANSITION
ENERGIES SUFFIXED BY C ARISE FROM CHANCE COINCIDENCE

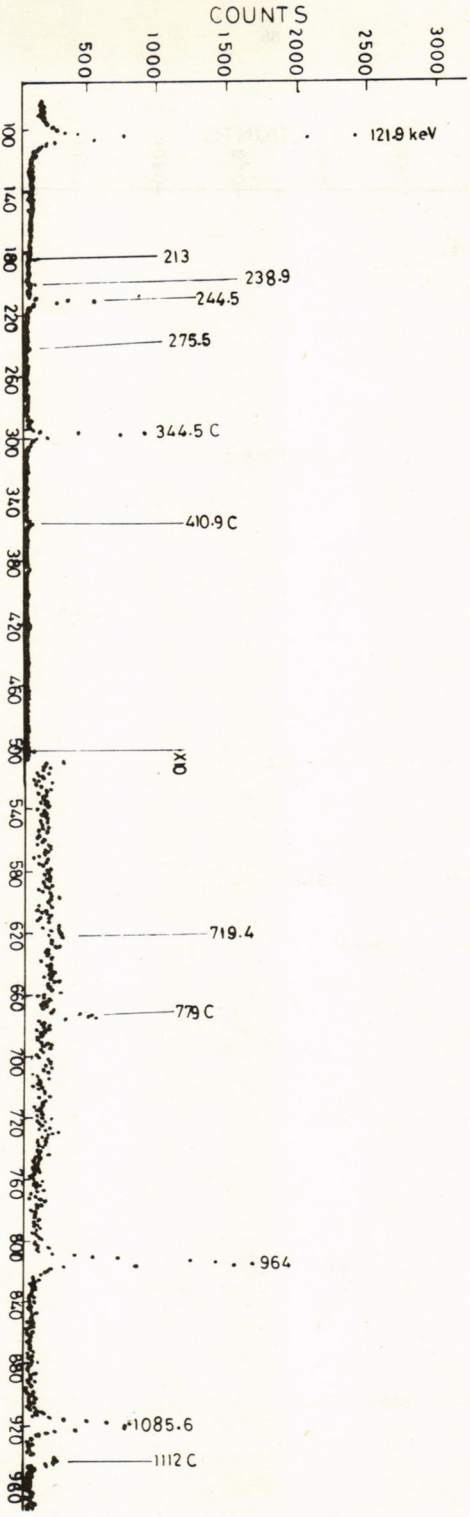

FIG.(9) GAMMA RAY SPECTRUM OF Eu^{152} IN COINCIDENCE WITH 444 KeV TRANSITION
ENERGIES SUFFIXED BY C ARISE FROM CHANCE COINCIDENCE

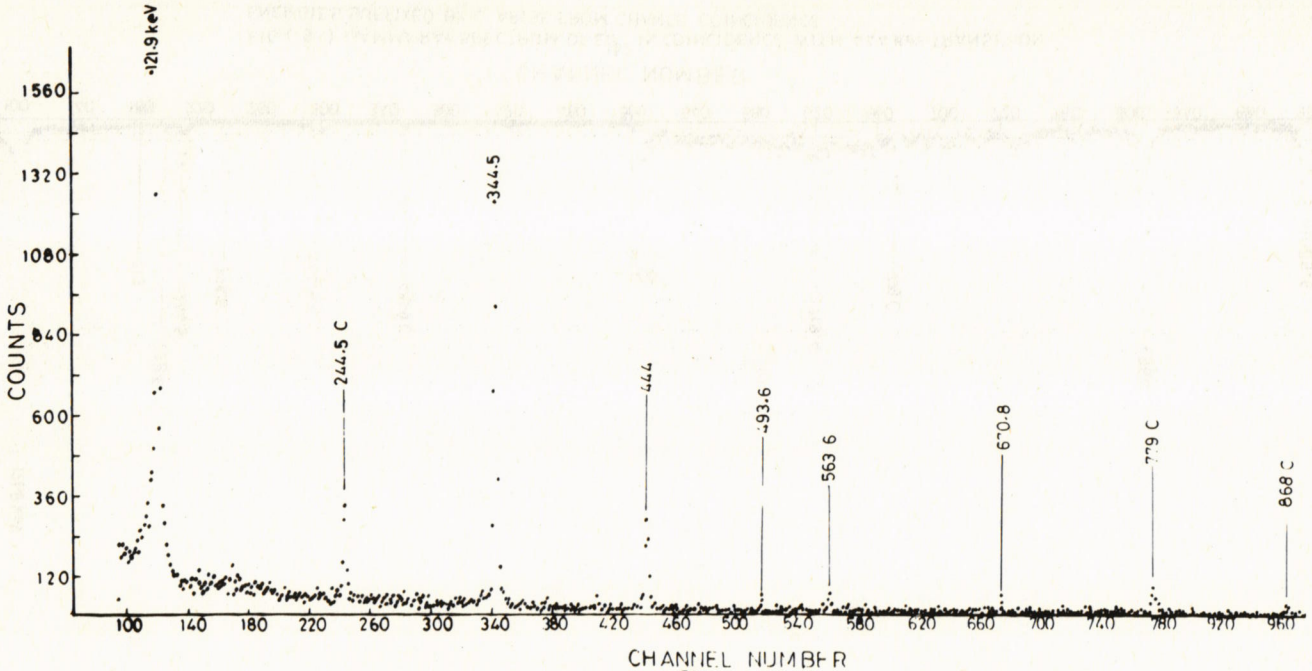

FIG(10) GAMMA RAY SPECTRUM OF Eu^{152} IN COINCIDENCE WITH 1085.9 KeV TRANSITION
ENERGIES SUFFIXED BY C ARISE FROM CHANCE COINCIDENCE. THE PRESENCE OF THE
STRONG 344.5 KeV PEAK DUE TO THE PARTIAL PRESENCE OF THE 1089 KeV γ RAY IN THE GATE

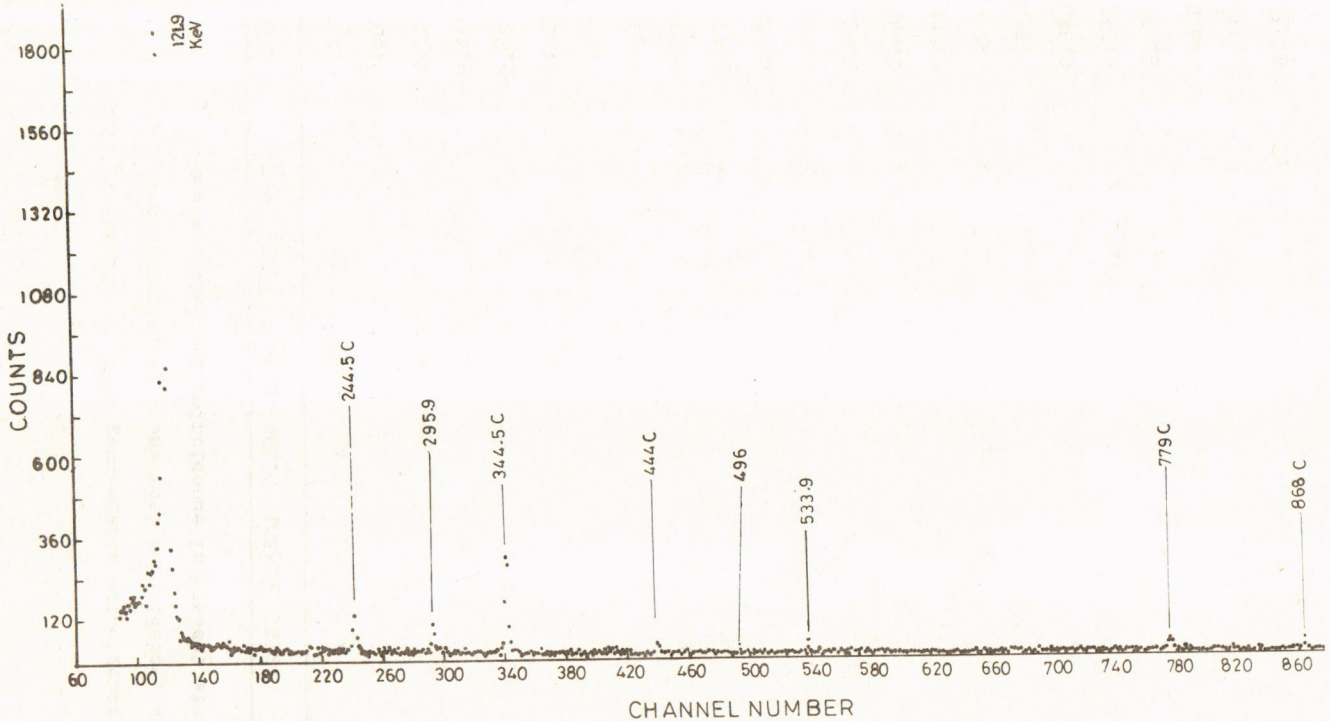

FIG.(11) GAMMA RAY SPECTRUM OF Eu^{152} IN COINCIDENCE WITH 1112 KeV TRANSITION
ENERGIES SUFFIXED BY C ARISE FROM CHANCE COINCIDENCE

Table 3. Results of ^{152}Sm gamma-gamma coincidence measurements. (x means real coincidence, and N means unobserved coincidence in present study).

Gate	121.9	244.5	444.0	964.0	1085.6	1112.0	1408.0
121.9		x	x	x		x	x
206.0							
213.0			x				
238.9			x				x
244.5	x						
251.0	x	x	x				
275.5		x					
285.9							
295.9	x	x				x	
329.8	x	x				N	
386.4							
416.0	x	x					
423.4							
444.0	x	x					
482.9							
488.3	x	x		x	x		
493.6							
496.0						x	
559.5		x					
563.6	x	x		N	x		
566.4				x			
613.9							
655.5	x	x					

Gate	121.9	244.5	444.0	964.0	1085.6	1112.0	1408.0
664.2		x					
670.8				x	x		
673.9	x	x					
688.7	x			x			
719.4	N	x	x				
723.0							
769.1	N	x	x				
810.7				N			
841.5	x	x					
868.0	x	x					
901.0	x						
919.3	x						
926.2	x	x					
964.0	x						
1006.0	x	x					
1085.6			x				
1112.0	x	x					
1212.3	x	x					
1250.0	x						
1363.7	x	N					
1390.8		x					
1408.0	x						
1458.6	x						
1529	x						

D. Search for Positrons

The energy difference between $^{152}Eu^{g}$ and ^{152}Sm is about 1.867 MeV which makes it possible to decay by a positron branch to the low-lying levels of ^{152}Sm, namely the 121.9 and 366.4 keV levels. This possibility is investigated by searching for 511-511 keV photon coincidences of the annihilation radiation. These coincidences are measured from a standard ^{22}Na source and from the ^{152}Eu source under the same conditions of location and energy gates. The coincidence count rates are recorded at both 90° and 180° angles, and the chance coincidences are calculated in all cases. The results obtained are used, together with the known activity of the standard ^{22}Na source, to calculate an estimate of the positron branching intensity which would be necessary to account for the observed annihilation radiation. The result obtained showed that the positron branch intensity is approximately equal to (0.016 ± 0.003) % of the total decay of ^{152}Eu. If the capture to positron ratio is considered it would imply that the electron capture transition intensity to the low-lying levels of ^{152}Sm is approximately equal to (2.46 ± 0.60) % which checks reasonably with the measured gamma intensities.

D I S C U S S I O N

^{152}Sm lies at the beginning of the deformed rare-earth region and displays the low-lying rotational energy bands. It is known as a "soft" nucleus (its VMI softness parameter [8]

is calculated to be 0.229). Figure 1 is a partial decay scheme of ^{152}Sm showing the main bands in its decay which are discussed below :

A. Ground-State Rotational Band

The energy levels at 0, 121.9, 366.4, and 706.9 keV have the well-known spin and parity of 0^+ , 2^+ , and 6^+ respectively. They belong to the ground-state rotational band with $K = 0^+$.

B. Beta-Vibrational Band

The energy levels at 684.8, 810.7, and 1023.6 keV have the spins and parities 0^+ , 2^+ , and 4^+ respectively. They are members of the beta-vibrational band with $K^\pi = 0^+$. These rotational levels are built over a beta-vibrational phonon with $\hbar\omega_B = 684.8$ keV. The anomalous branching ratio out of the beta-vibrational band [7] has been studied by Kumar using the pairing-plus-quadrupole (PPQ) model, and by Stokstad who calculated successfully the E2 matrix elements of the beta-ground transitions.

C. Gamma-Vibrational Band

The energy levels at 1085.6, 1233.9, and 1371.9 keV have the spins and parities 2^+ , 3^+ , and 4^+ respectively. They are members of the gamma-vibrational band with $K^\pi = 2^+$. The gamma-vibrational levels decay to the levels of the ground

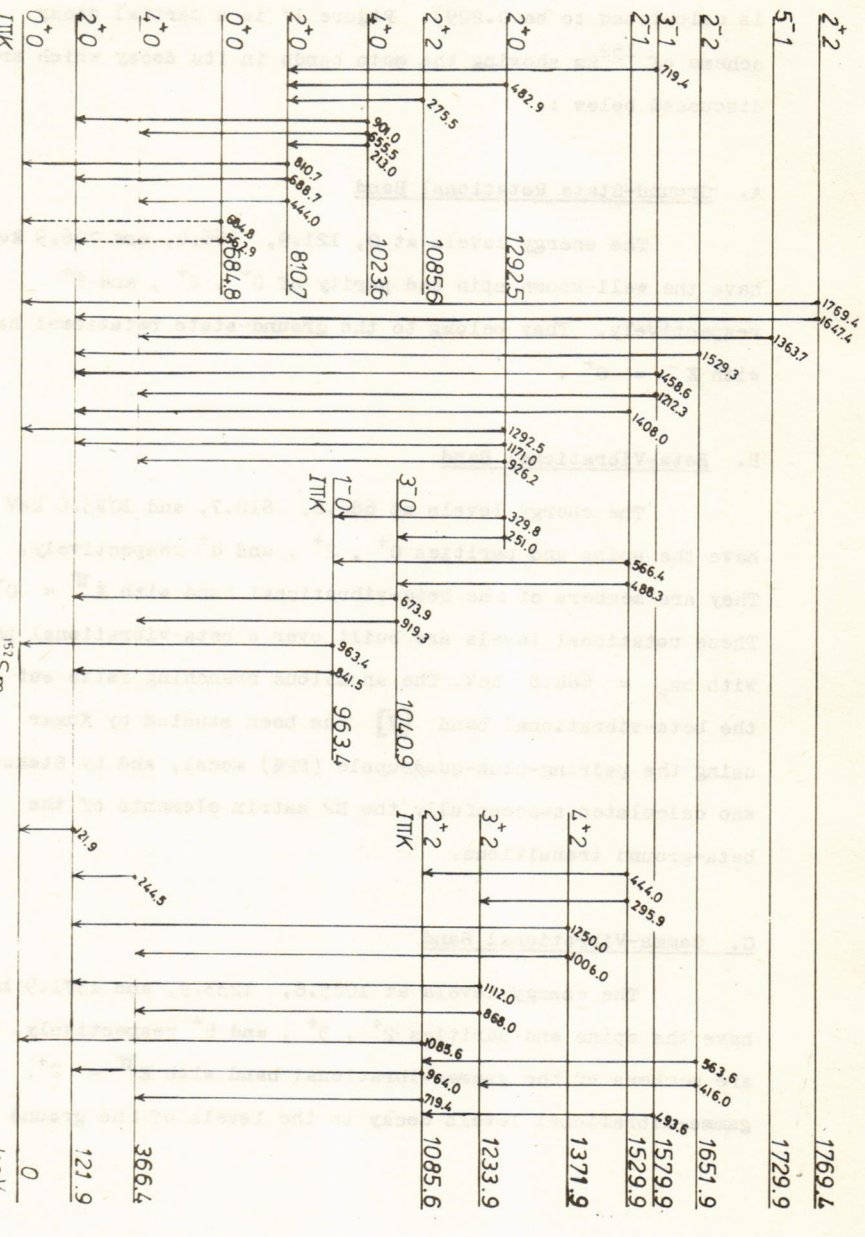

FIG. (12) BAND LEVEL SCHEME OF ^{152}Sm. DASHED LINES INDICATE UNOBSERVED TRANSITIONS.

state band and also to the 2^+ beta-band level, these transitions demonstrate the gamma-ground and gamma-beta mixing. The transitions intensities and the B(E2) values for the gamma-beta inter-band transitions have been compared [7] with the predictions of PPQ model, the results are not always satisfactory.

D. Octupole-Vibrations Band

The 963.4 and 1040.9 keV levels belong to the $K^{\pi} = 0^-$ octupole vibrations band, they are assigned spins and parities of 1^- and 3^- respectively. A 5^- level reported [9] at 1222 keV has not been observed and cannot be confirmed in the radioactive decay of ^{152}Sm. The 963.4 keV level is strongly populated [5 - 9] in the decay of $^{152}Eu^m$ and is much less in the decay of $^{152}Eu^g$. This level is only fed by gamma transitions deexciting the higher levels.

E. Higher Energy States

(i) The 1529.9 and 1579.9 keV levels are the 2^- and 3^- members of the $K^{\pi} = 1^-$ band. The collective nature of the 2^- level is supported by angular correlation experiments [10] where it is found that the transition from the 3^- member of the octupole vibrations band has an E2 nature. The 1^- member of this band is reported [9] at 1510.8 keV which is excited in the decay of $^{152}Eu^m$ but is not observed in the decay of $^{152}Eu^g$. The 5^- member of this band is assigned at 1726 keV through inelastic deuteron scattering experiments [2] but it is not observed in the decay of ^{152} Eu.

(ii) The 1292.5 level seems of particular interest since there is some evidence [11] that ^{152}Sm nucleus has, in this state, a smaller deformation than in the ground state, i.e., the 1292.5 level is almost a spherical state. The decay of this level is preferentially to the levels of the g.s. band, beta band, and octupole rotational band, but no gamma transitions to the gamma-vibrational band. Therefore, it is suggested that this level is the 2^+ member of a two-phonon beta-vibrational band. In the decay of $^{152}Eu^m$, a 0^+ member of this band is observed at 1082.8 keV but it is not present in the decay of $^{152}Eu^g$,

(iii) The 1651.9 and 1757.2 keV levels are confirmed by coincidence measurements and they display similar features. The 1651.9 keV level is assigned a spin of 2^- and is considered as the band head of a new octupole band with $K^\pi = 2^-$; this assignment is supported by the relative B(E1) values [9] of the transitions deexciting this level. The 1757.2 keV level is another member of the same band it is assigned a spin of 3^+ by Barrette et al. [9] on grounds of its decay characteristics.

(iv) The 1680 keV level is reported due to the coincidence measurements. It is assigned a spin of 1^- based on the decay characteristics and the log ft value. The 1701.4 keV level is proposed to explain the very weak coincidence between 244.5 and 1334.7 keV lines. The decay of this level only to the 4^+ state of the g.s. band indicates that

its spin is 4^- or 5^-. The 1769.4 keV level is suggested [9] to be a coupled beta-gamma two-phonon 2^+ state based on the energy sum of 0^+ beta level and 2^+ gamma level.

CONCLUSIONS

The investigation of the decay characteristics of $^{152}Eu^g$ has revealed the existence of 58 gamma transitions in the decay of ^{152}Sm where twenty excited states have been confirmed, and the decay scheme has been proposed. Several states are confirmed in this investigation by coincidence results while they have been placed before by energy fit alone. The positron branch from ^{152}Eu to the low-lying levels of ^{152}Sm is measured to be equal to (0.016 ± 0.003) % by measuring the annihilation radiation coincidences. The electron capture branch is estimated to be about (2.46 ± 0.6) % of the total decay of $^{152}Eu^g$. The intensities of the very weak transitions between the different bands have been measured. The comparison of the inter-band transitions intensities with the predictions of different theoretical models is not always satisfactory, and further investigations are needed to explore the anomalous branching ratios between different bands.

REFERENCES

1. Nuclear Data Sheets (1479) 5-6-37, (1964).
2. E.Veje, B. Elbek, B. Herskind, and M.C. Oslen; Nucl. Phys. A - 109, 489 (1968).
3. O. Lonsjo and G.B. Hagemann; Nucl. Phys. 88. 624 (1966).
4. G.G. Seaman, J.S. Greenberg, D.A. Bronely, and F.K. McGowan; Phys. Rev. 149, 925 (1966).
5. L.L. Reidinger, N.R. Johnson, and J.H. Hamilton; Phys. Rev. C2 2358 (1970).
6. L.Varnell, J.D. Bowman and J. Tresehuk; Nucl. Phys. A 127, 270 (1969).
7. K.R. Baker, J.H. Hamilton, and A.V. Ramyya; Z. Physik 256, 387 (1972).
8. M.A.J. Mariscotti, G. Scharff-Goldhaber, and B. Buck; Phys. Rev. 178, No.4, 1864 (1969).
9. J. Barrette, M. Barrette, A. Boutard, G. Lamoureux, S. Monaro, and Z. Markiza; Can. J. Phys. 49, 2462 (1971).
10. J. Barrette, M. Barrette, A. Boutard, G. Lamoureux, and S. Monaro; Can. J. Phys. 48, 2011 (1970).
11. J.S. Larsen, O. Skilbreid, and L. Visiren ; Nucl. Phys. A 100, 248 (1967).
12. R.A. Meyer, Phys. Rev. 174, 1478 (1968).

مجلة علوم المستنصرية

١٩٨٠

رقم الايداع في المكتبة الوطنية ٢٧٨ لسنة ١٩٨٠

مجلة علوم المستنصرية

المجلد ٥ العدد ١ ، ١٩٨٠

كلية العلوم — الجامعة المستنصرية — بغداد — العراق

تعليمات للمؤلفين

١. تقدم ثلاث نسخ من البحث مطبوعة على الآلة الكاتبة وعلى ورق ابيض صقيل وتترك مسافة ٢,٥ سم على يسار كل صفحة .

٢. تقدم خلاصة باللغة العربية وأخرى باللغة الانكليزية وتطبع كل منهما على ورقة منفصلة .

٣. يطبع عنوان البحث وكذلك اسم المؤلف (او المؤلفين) وعنوانه على ورقه منفصلة ويكتب اسم المؤلف كاملا كان يكتب (احمد م. علي) .

٤. تقدم الرسوم التوضيحية منفصلة عن مسودة البحث وترسم بالحبر الصيني الاسود على ورق شفاف وترفق ثلاث صور لكل رسم وتكتب عناوين الرسوم على نفس الورقة .

٥. تنظم الجداول باسلوب تجعلها مفهومة دون اللجوء الى النص وذلك باعطاء كل جدول وكل عمود وصفا واضحا .

٦. لايجوز اعطاء المعلومات ذاتها بالرسم وبالجدول في وقت واحد الا اذا اقتضت ضرورة النقاش ذلك .

٧. يشار الى المصدر برقم ضمن قوسين [ ] بعد الجملة مباشرة وتطبع كافة المصادر على ورقة منفصلة

٨. من المجد حيثما كان ممكنا ان يتسلسل البحث ليتضمن المقدمة ، طرق التجربة ، النتائج . المناقشة .

مجلة علوم المستنصرية

المجلد ٥ العدد ١ حزيران ١٩٨٠

مطبعة اوفسيت باسم ☎ ٨٨٨٧٥٤٥